Advanced Review

Vibrational circular dichroism

Gábor Magyarfalvi,* György Tarczay* and Elemér Vass*

This review focuses on the theoretical background of vibrational circular dichroism (VCD) spectroscopy. Besides discussing the first-principle approaches of the theoretical evaluation of VCD spectra, practical computational considerations, such as the available electronic structure computational levels and program packages, are summarized. Illustrative examples are shown for the absolute configuration and conformation determination of mid-sized molecules based on the comparison of calculated end experimental VCD spectra, including the comparison of the performance of different computational levels. The conformational analysis of larger biomolecules, such as carbohydrates, nucleotides, and peptides by VCD spectroscopy, and the theoretical simulation of solvent effects are also discussed. The review is concluded by a short summary of the present stage of the computation of VCD spectra and the expected future direction of theoretical developments. *WIREs Comput Mol Sci* 2011 1 403–425 DOI: 10.1002/wcms.39

INTRODUCTION

The vibrational circular dichroism (VCD) technique is very closely related to the more well-known electronic circular dichroism (ECD) spectroscopy both from theoretical and experimental points of view. In spite of the very close relationship, the VCD technique has numerous advantages over the ECD spectroscopy. First, the investigated chiral molecules do not need to have any chromophoric groups. Second, VCD spectra have a richer structural content, thus the main application of these methods, i.e., the determination of absolute configuration can be based on more assigned bands. Third, in the case of flexible molecules the higher resolution allows the simultaneous determination of configuration and conformation. Finally, the first principles evaluation of VCD spectra can be carried out more reliably; hence the probability of an incorrect interpretation is much smaller than in the case of ECD spectroscopy.

VCD spectroscopy has become one of the most powerful tools for the determination of the absolute configuration of chiral molecules in the new millennium. In addition to the advantages listed above, this progress can be attributed to the availability of commercial VCD spectrometers from the late 1990s, to the decisive theoretical and experimental developments of the 1980s and 1990s and to the implementation of theoretical models into widely used quantum chemical program packages. As a proof of the success of this method, the number of VCD studies published has increased an order of magnitude during the last ten years.

Although nowadays computer codes are often used as black-box tools when calculating VCD spectra, in order to avoid wrong interpretations users have to keep in mind the approximations used and the factors neglected by the theoretical approach selected, as well as the performance and limits of the computational method applied. It is hoped that this review can guide both theoreticians and experimentalists who are familiarizing themselves with the field of VCD spectroscopy and its applications.

Theoretical Background

The fundamental theory behind differential absorption of circularly polarized light by enantiomeric pairs of chiral molecules (circular dichroism) is not specific to vibrational excitations. Rosenfeld's general formula[1] published in 1928 is equally relevant to all forms of circular dichroism (in the case of randomly oriented samples). The difference in absorption is proportional to the rotational strength, R_{ab} belonging to the transition from state 'a' to state 'b':

$$R_{ab} = \mathrm{Im}\{\langle a|\boldsymbol{\mu}_e|b\rangle\langle b|\boldsymbol{\mu}_m|a\rangle\}, \quad (1)$$

*Correspondence to: gmagyarf@chem.elte.hu; tarczay@chem.elte.hu; evass@chem.elte.hu

Institute of Chemistry, Eötvös Loránd University, Budapest, Hungary

DOI: 10.1002/wcms.39

where $\boldsymbol{\mu}_e$ and $\boldsymbol{\mu}_m$ are the electric and magnetic dipole operators of the molecular system:

$$\boldsymbol{\mu}_e = \sum_k q_k \mathbf{r}_k \; \boldsymbol{\mu}_m = \frac{1}{2c} \sum_k q_k \mathbf{r}_k \times \mathbf{p}_k. \qquad (2)$$

Here q_k, $\mathbf{r}_k$, and $\mathbf{p}_k$ stand for the charge, the position operator, and momentum operator of the kth particle of the molecular system, including nuclei and electrons. Here, and in other equations, we use atomic units and the Gaussian CGS unit convention for electromagnetic quantities simplifying most formulas. These are the equations internally used by the computer codes; results are converted to conventional units only at the end of the computations.

This formula explains several well-known properties of experimental VCD spectra. Although the electric dipole operator and the magnetic dipole operator have a different symmetry character (i.e., odd or even) under reflection or inversion, their product, the predicted rotational strength is odd and will change sign upon the symmetry operation. Thus the computed results for the vibrations of enantiomeric pairs will yield VCD intensities of equal magnitude and opposite sign as observed experimentally.

The alternating sign means that the rotational strength for symmetric molecules (containing at least an axis of improper rotation) must be zero. This disappearing rotational strength comes from the scalar product of two transition moment vectors. Unless either transition moment is zero, these vectors must be perpendicular to each other in achiral, i.e., VCD inactive molecules.

The sum of rotational strengths of all fundamental vibrational frequencies can also be shown to be zero using the closure relation running over excited vibrational states (v) on and the perpendicularity of the two dipole operators:

$$\sum_v R_{0v} = \mathrm{Im}\left\{\sum_v \langle 0|\boldsymbol{\mu}_e|v\rangle\langle v|\boldsymbol{\mu}_m|0\rangle\right\}$$
$$= \mathrm{Im}\{\langle 0|\boldsymbol{\mu}_e\boldsymbol{\mu}_m|0\rangle - \langle 0|\boldsymbol{\mu}_e|0\rangle\langle 0|\boldsymbol{\mu}_m|0\rangle\} = 0. \qquad (3)$$

Rosenfeld's formula Eq. (1) is misleadingly simple, but its evaluation based on first principles is far from being straightforward. In ECD, only the electronic terms of the transition moment operators are important, as in computations excitations can be generally regarded vertical making the nuclear term insignificant (see Ref 2, for further details).

In VCD, both nuclear and electronic terms are important and especially the evaluation of the electronic terms of the magnetic transition dipole is not obvious. That could explain why reliable first principles calculations lagged somewhat behind similar molecular properties and were only implemented relatively late. The theory behind these calculations was worked out in the 1980s, approximately 10 years after the first experimental detection[3–5] of vibrational circular dichroism. The experimental work also required significant technical developments, since molecular VCD is an intrinsically weak phenomenon, the differential absorptions being several orders of magnitude smaller than infrared absorptions.

The theoretical approaches for computation of rotational strength are conveniently discussed in terms of the two kinds of transition dipoles.

Atomic Polar Tensors

Of the two factors of the rotational strength, the evaluation of the electric transition dipoles has a long established history in vibrational absorption spectroscopy, since the intensities of infrared absorption bands are determined by the dipole strengths, the square of the electric transition dipoles. A ubiquitous approach is the use of the double harmonic approximation. That means that both the potential energy surface and the dipole surfaces are simplified in the vicinity of the minimum to quadratic and linear surfaces, respectively. Behind the existence of these surfaces is another prerequisite condition, the Born–Oppenheimer (BO) approximation.

The BO approximation supposes that the molecular wave function (Φ) is a simple product of the nuclear (ξ) and electronic (ψ) wave functions. Vibrational spectra are predicted using harmonic oscillator solutions for individual normal modes of the nuclear motion problem. The electric transition dipole moment for a fundamental vibrational transition in this context can be evaluated expanding the dipole moment in terms of the mass weighted normal coordinate (Q_j) up to first order:

$$\langle \psi_0\xi_1|\boldsymbol{\mu}_e|\psi_0\xi_0\rangle = \left\langle \xi_1 \middle| \langle\psi_0|\boldsymbol{\mu}_e|\psi_0\rangle_{Q=0} + \left(\frac{\partial\langle\psi_0|\boldsymbol{\mu}_e|\psi_0\rangle}{\partial Q_j}\right)_{Q=0} Q_j \middle| \xi_0 \right\rangle$$
$$= \left(\frac{1}{2\omega_j}\right)^{1/2} \left(\frac{\partial\langle\psi_0|\boldsymbol{\mu}_e|\psi_0\rangle}{\partial Q_j}\right)_{Q=0}. \qquad (4)$$

The simplifications of the last step make use of the harmonic oscillator nuclear wave functions that are orthogonal to each other and the angular frequency (ω_j) of the jth vibrational normal mode. Most

often the dipole derivatives appearing in the result are analyzed with the help of the so-called atomic polar tensors (APTs).[6] These tensors are defined as molecular dipole derivatives with respect to the Cartesian coordinates ($\mathbf{R}_i$) of individual nuclei evaluated at the equilibrium structure, indicated as $R = 0$ or equivalently $Q = 0$.

$$\mathbf{T}_i = \left(\frac{\partial\langle\psi_0|\boldsymbol{\mu}_e|\psi_0\rangle}{\partial\mathbf{R}_i}\right)_{R=0} = \begin{pmatrix} \left(\frac{\partial\langle\psi_0|\mu_{e,x}|\psi_0\rangle}{\partial R_{i,x}}\right)_{R=0} & \left(\frac{\partial\langle\psi_0|\mu_{e,x}|\psi_0\rangle}{\partial R_{i,y}}\right)_{R=0} & \left(\frac{\partial\langle\psi_0|\mu_{e,x}|\psi_0\rangle}{\partial R_{i,z}}\right)_{R=0} \\ \left(\frac{\partial\langle\psi_0|\mu_{e,y}|\psi_0\rangle}{\partial R_{i,x}}\right)_{R=0} & \left(\frac{\partial\langle\psi_0|\mu_{e,y}|\psi_0\rangle}{\partial R_{i,y}}\right)_{R=0} & \left(\frac{\partial\langle\psi_0|\mu_{e,y}|\psi_0\rangle}{\partial R_{i,z}}\right)_{R=0} \\ \left(\frac{\partial\langle\psi_0|\mu_{e,z}|\psi_0\rangle}{\partial R_{i,x}}\right)_{R=0} & \left(\frac{\partial\langle\psi_0|\mu_{e,z}|\psi_0\rangle}{\partial R_{i,y}}\right)_{R=0} & \left(\frac{\partial\langle\psi_0|\mu_{e,z}|\psi_0\rangle}{\partial R_{i,z}}\right)_{R=0} \end{pmatrix}. \quad (5)$$

APTs can be transformed to normal coordinate derivatives using the displacement vectors ($\mathbf{S}_{i,j}$) of individual nuclei:

$$\mathbf{S}_{i,j} = \left(\frac{\partial\mathbf{R}_i}{\partial Q_j}\right)_{Q=0}$$

$$d\mathbf{R}_i = \sum_j \mathbf{S}_{i,j} dQ_j \left(\frac{\partial\langle\psi_0|\boldsymbol{\mu}_e|\psi_0\rangle}{\partial Q_j}\right)_{Q=0} = \sum_i \mathbf{T}_i \mathbf{S}_{i,j}. \quad (6)$$

The dipole moment operator in the definition of the APTs includes nuclear and electronic terms that can be evaluated separately (α and $\beta \in \{x, y, z\}$, where x, y, z are Cartesian coordinates):

$$\mathbf{T}_{i,\alpha\beta} = Z_i\delta_{\alpha\beta} + 2\left\langle\left(\frac{\partial\psi_0}{\partial R_{i,\alpha}}\right)_{R=0}|\mu_{e,\beta}|\psi_0\right\rangle. \quad (7)$$

The part of the APT tensors from the nuclear dipole momenta is a simple tensor containing the nuclear charge (Z_i) in all three diagonal positions. The electric contribution to the APT tensors, or differently the dipole derivatives are implemented in many electronic structure programs and can be evaluated at several levels of accuracy with respect to electron correlation (HF, DFT, MP2, CCSD, etc.). Their calculation is usually linked with the computation of the force constants that are required to predict the normal modes and harmonic vibrational frequencies. Analytical derivatives of the electronic wave functions with respect to nuclear coordinates are needed to evaluate the force constants and the APTs.

The dipole derivatives can be regarded as second derivatives of the molecular energy (ε) with respect to nuclear coordinates and a hypothetical external electric field (E). Analytical derivative codes make use of this paradigm in the evaluation of APTs:

$$\mathbf{T}_{i,\alpha\beta} = -\left(\frac{\partial^2\varepsilon}{\partial\mathbf{R}_{i,\alpha}\partial\mathbf{E}_\beta}\right)_{R=0}. \quad (8)$$

Atomic Axial Tensors

The magnetic dipole transition moment behaves differently from the electric transition moment. When the electronic wave function can be chosen real, as is the case with nondegenerate singlet electronic states, the expectation value of the purely imaginary and Hermitian magnetic dipole operator for the electronic ground state is necessarily zero. This fact remains unchanged when the nuclear configuration changes, thus there is no magnetic dipole surface, and there is no electronic contribution to the magnetic transition dipole.

The lack of the electronic contribution is obviously unphysical and stems from the inadequacy of the BO approximation in this case. The BO approximation takes account of the effect of the nuclear position on the electronic wave function parametrically, but the effect of the nuclear motion on the electrons is completely neglected. It is worth noting that the same neglect makes the BO wave functions inadequate to describe the electric transition dipoles if the dipoles are evaluated in the dipole velocity formalism[7] instead of the ubiquitous dipole length formalism.

A number of heuristic theories were worked out previously (Coupled Oscillator,[8] Fixed Partial Charges,[9] Localized Molecular Orbital,[10] etc.) to give nonvanishing magnetic transition momenta and rotational strengths, but the definitive approach was to go beyond the BO approximation. That was the route started by the vibronic coupling theory (VCT) of Nafie and Freedman[11] that uses a perturbational mixing of BO-type product wave functions of electronic and vibrational states. VCT theory results in a sum-over-states (SOS) expression that is more challenging for practical computations since in principle

the calculation includes a summation for all electronic excited states.

The critical step toward the reliable evaluation of rotational strength was taken by Stephens[12] by introducing the magnetic field perturbation (MFP) approach. This work has identified an expression for the electronic part of the magnetic transition moment that is based on analytical derivatives and requires only a good description of the electronic ground state.

Buckingham et al.[13] almost simultaneously have arrived to similar results by defining and using molecular property surfaces that are dependent on nuclear velocities or momenta instead of the more easily visualized surfaces that change with nuclear positions. Looking at the gradients of these surfaces can circumvent the shortcomings of the BO approximation. If the magnetic transition moment is expanded in the momentum associated with a normal coordinate (so-called conjugate momentum, W_j) close to the equilibrium position, only the odd terms remain:

$$\begin{aligned}&\langle\psi_0\xi_1|\boldsymbol{\mu}_\mathrm{m}|\psi_0\xi_0\rangle\\&=\left\langle\xi_1\left|\left(\frac{\partial\langle\psi_0|\boldsymbol{\mu}_\mathrm{m}|\psi_0\rangle}{\partial W_j}\right)_{Q=0}\left(\frac{\partial W_j}{\partial Q_j}\right)_{Q=0}Q_j\right|\xi_0\right\rangle\\&=i\left(\frac{\omega_j}{2}\right)^{1/2}\left(\frac{\partial\langle\psi_0|\boldsymbol{\mu}_\mathrm{m}|\psi_0\rangle}{\partial W_j}\right)_{Q=0}.\end{aligned}\tag{9}$$

The nuclear wave function is again supposed to be harmonic, with an angular frequency of ω_j. The magnetic dipole transition moment is purely imaginary in this approximation. A similar argument based on velocity derivatives was first introduced by Nafie.[14]

Analogously to APTs, Stephens has introduced[15] the so-called atomic axial tensors (AATs) that can be defined as derivatives of the molecular magnetic moment with respect to individual nuclear momenta (P_j).

$$\mathbf{M}_i=\left(\frac{\partial\langle\psi_0|\boldsymbol{\mu}_\mathrm{m}|\psi_0\rangle}{\partial\mathbf{P}_i}\right)_{Q=0}=\begin{pmatrix}\left(\frac{\partial\langle\psi_0|\mu_{\mathrm{m,x}}|\psi_0\rangle}{\partial P_{i,\mathrm{x}}}\right)_{Q=0}&\left(\frac{\partial\langle\psi_0|\mu_{\mathrm{m,x}}|\psi_0\rangle}{\partial P_{i,\mathrm{y}}}\right)_{Q=0}&\left(\frac{\partial\langle\psi_0|\mu_{\mathrm{m,x}}|\psi_0\rangle}{\partial P_{i,\mathrm{z}}}\right)_{Q=0}\\\left(\frac{\partial\langle\psi_0|\mu_{\mathrm{m,y}}|\psi_0\rangle}{\partial P_{i,\mathrm{x}}}\right)_{Q=0}&\left(\frac{\partial\langle\psi_0|\mu_{\mathrm{m,y}}|\psi_0\rangle}{\partial P_{i,\mathrm{y}}}\right)_{Q=0}&\left(\frac{\partial\langle\psi_0|\mu_{\mathrm{m,y}}|\psi_0\rangle}{\partial P_{i,\mathrm{z}}}\right)_{Q=0}\\\left(\frac{\partial\langle\psi_0|\mu_{\mathrm{m,z}}|\psi_0\rangle}{\partial P_{\mathrm{i,x}}}\right)_{Q=0}&\left(\frac{\partial\langle\psi_0|\mu_{\mathrm{m,z}}|\psi_0\rangle}{\partial P_{i,\mathrm{y}}}\right)_{Q=0}&\left(\frac{\partial\langle\psi_0|\mu_{\mathrm{m,z}}|\psi_0\rangle}{\partial P_{i,\mathrm{z}}}\right)_{Q=0}\end{pmatrix}.\tag{10}$$

Transformation of nuclear momenta to the conjugate momentum of normal modes is carried out using the same displacement vectors:

$$\begin{aligned}\mathbf{S}_{i,j}&=\left(\frac{\partial\mathbf{P}_i}{\partial W_j}\right)_{Q=0}=\left(\frac{\partial\mathbf{R}_i}{\partial Q_j}\right)_{Q=0}\\d\mathbf{P}_i&=\sum_j\mathbf{S}_{i,j}dW_j\left(\frac{\partial\langle\psi_0|\boldsymbol{\mu}_\mathrm{m}|\psi_0\rangle}{\partial W_j}\right)_{Q=0}=\sum_i\mathbf{M}_i\mathbf{S}_{i,j}.\end{aligned}\tag{11}$$

The AATs are also composed of two parts, based on the magnetic moment operator in Eq. (2) applied to nuclei and electrons. The nuclear part makes use of the Levi-Civita symbol ($\varepsilon_{\alpha\beta\gamma}$), but is rather simple, while the electronic part needs more consideration:

$$\mathbf{M}_{i,\alpha\beta}=\frac{Z_i}{2c}\sum_\gamma\varepsilon_{\alpha\beta\gamma}\mathbf{R}_{i,\gamma}+\left(\frac{\partial\langle\psi_0|\boldsymbol{\mu}_\mathrm{m}|\psi_0\rangle}{\partial\mathbf{P}_i}\right)_{Q=0}.\tag{12}$$

The magnetic dipole derivative can be regarded as a second derivative of the molecular energy (ε) with respect to nuclear momenta ($\mathbf{P}_i$) and the external magnetic field ($\mathbf{B}$). As the ground state electronic wave function has no implicit dependence on the nuclear momenta, only the total molecular Hamiltonian (the nuclear kinetic energy term) contributes to the derivative with respect to the momenta:

$$\begin{aligned}-\left(\frac{\partial^2\varepsilon}{\partial\mathbf{P}_{i,\alpha}\partial\mathbf{B}_\beta}\right)_{Q=0,\mathbf{B}=0}&=-\left(\frac{\partial\langle\psi_0|\frac{\partial\widehat{H}}{\partial\mathbf{P}_{i,\alpha}}|\psi_0\rangle}{\partial\mathbf{B}_\beta}\right)_{Q=0,\mathbf{B}=0}\\&=-\left(\frac{\partial\langle\psi_0|-i\frac{\partial}{\partial\mathbf{R}_{i,\alpha}}|\psi_0\rangle}{\partial\mathbf{B}_\beta}\right)_{Q=0,\mathbf{B}=0}\\&=2i\left\langle\frac{\partial\psi_0}{\partial\mathbf{B}_\beta}\middle|\frac{\partial\psi_0}{\partial\mathbf{R}_{i,\alpha}}\right\rangle_{Q=0,\mathbf{B}=0}.\end{aligned}\tag{13}$$

In the second step, we made use of the fact that the nuclear kinetic energy is quadratic in the

nuclear moment. The final result is practically identical to Stephens' seminal formula[12] that enabled the reliable first principles calculation of rotational strengths. AATs as defined here contain an extra factor of $2i$ following Nafie,[16] making the tensor components real values, and giving a plausible interpretation of the tensor (magnetic dipole derivative with respect to nuclear momenta).

AATs, like magnetic momenta are gauge dependent.[15] If the origin of the coordinate is transformed with a translation vector $\mathbf{Y}$, magnetic momenta and AATs are transformed to the new gauge and change:

$$\mathbf{M}'_{i,\alpha\beta} = \mathbf{M}_{i,\alpha\beta} - \frac{1}{2c}\sum_{\gamma\delta}\varepsilon_{\beta\gamma\delta}\mathbf{Y}_{\gamma}\mathbf{T}_{i,\delta}. \qquad (14)$$

The transformation uses the APTs. Only the rotational strength, the final result of a VCD calculation is a gauge invariant physical observable.

To evaluate AATs, Stephens' formula[12] requires electronic wave function derivatives with respect to nuclear positions and magnetic flux densities. The former are produced in the calculation of the force constants and are available during a vibrational analysis. Magnetic field derivatives are produced when second-order magnetic properties (e.g., magnetic nuclear shieldings or magnetic susceptibilities) are calculated. To implement VCD intensities using Stephens' formula Eq. (13), these two computations need to be combined. Usually, the calculation of the force constants dominates the computational time requirements of the VCD calculations.

COMPUTATIONAL METHODS

A crucial point in evaluating molecular magnetic properties, including AATs, is the accurate description of the response of the electronic wave function to a magnetic field. The magnetic field derivatives of the normally real valued electronic wave function are purely imaginary quantities since the magnetic perturbation operator (magnetic dipole operator) is also purely imaginary. This operator is the generator of infinitesimal rotations around the origin of the coordinate system. Normal basis sets are not well adapted to describe these rotations, especially if the nucleus studied is not placed at the origin. Thus the use of a finite basis introduces gauge dependent errors unless a very large basis set is used.

Two common strategies exist to rectify the situation for AAT calculations. If individual AATs are evaluated in a coordinate system centered on each nucleus and transformed to a common origin using Eq. (14), the gauge dependent errors are reduced greatly. This distributed origin (DO) gauge was proposed by Stephens[15] and was implemented in *ab initio* calculations (in the CADPAC program package) with markedly improved accuracy over common origin calculations.[17]

The gauge dependent error is also eliminated if the perturbing effect is explicitly included in the description of the wave function (as the nuclear motion is included through the nucleus centered basis functions). One method that applies magnetic field dependent phase factors to localized molecular orbitals is LORG (local orbital/local origin) of Bouman and Hansen.[18] Although VCD results were promising,[19] the method was not adapted widely.

The ubiquitous solution to the gauge problem is the use of magnetic field dependent basis functions, the so-called Gauge Including Atomic Orbitals (GIAOs)[20] or London basis sets.[21] Using GIAOs moderately large basis sets are known to give reasonably accurate rotational strengths. This is the method of choice in actively developed quantum chemistry program packages that implement VCD rotational strength calculations. By far the most widespread choice is Gaussian[22] that was the first program to provide fast and reliable results using density functional theory.[23] Dalton[24] is another code that is the descendant of the first GIAO-HF and GIAO-MCSCF VCD capable program.[25] Other program packages that implement VCD rotational strengths are ADF[26] (Amsterdam Density Functional software, density functional only) and PQS[27] (Parallel Quantum Solutions software, HF, and DFT).

The first *ab initio* evaluations[28] of vibrational rotational strengths were carried out using uncorrelated (HF) wave functions. The effect of correlation on the quality of results was not surveyed extensively. Sets of calculations were published using MP2[29] and MCSCF[25] theory. The results showed improvements compared to HF calculations, but at an excessive computational cost. The wide adoption of DFT in the 1990s had brought the dominance of DFT calculations in the study of VCD intensities.[23] These computations provide reasonably accurate results with moderate computational cost.

The lack of detailed studies on correlation may be due to the fact that the significance of the numerical accuracy of rotational strengths is not very high. Quite often a qualitative agreement in the signs and magnitude of individual VCD bands is sufficient to interpret the spectra. The evaluation of AATs using higher level, such as coupled cluster wave functions would require considerable programming and computational effort. It is still a possibility though to

evaluate AATs at a lower theoretical level, and the APTs and force constants at a higher level.[30] Such calculations violate the exact gauge independence of rotational strengths, but show at least a part of the effect of correlation.

In addition to electron correlation, a major source of inaccuracy could come from the simplifications in the derivation of APTs and AATs. The central assumption is the use of the double harmonic approximation. This theory does not allow for overtones or combination bands, although VCD activity can be detected in this spectral region as well.[31] Large-amplitude motions are also unlikely to be well described as harmonic motion. There were attempts to calculate rotational strengths for anharmonic vibrations[32] but the method is not in general use. The linear change of the magnetic transition moment with the nuclear momenta is probably a good approximation, since only the linear and cubic terms are present; the quadratic terms are zero due to symmetry reasons. It is worth noting that the BO approximation was not invoked during the derivation of the formula for AATs, thus no inaccuracy is introduced when the calculation is based on the ground state electronic wave function.

Another deficiency in the derivation is that it does not allow for molecules with inherent magnetic momenta, such as radicals or transition metal complexes. The latter can show abnormal rotational strengths,[33] and supposedly low-lying electronic states are responsible[34] for the unusually strong VCD bands.

In the interpretation of VCD spectra, the correct signs are crucial when assigning absolute conformation, while the accuracy of the magnitude of the rotational strengths is less important. Nicu et al. introduced a very useful concept[35] that would classify calculated VCD bands depending on their response to slight changes in the computational method. If a band could easily change sign upon a minor change in molecular geometry or basis set, then these so-called nonrobust modes should be disregarded and only the so-called robust bands are to be assigned. Unfortunately, the measure selected by the authors, the angle between the electric and magnetic transition moment vectors is not optimal. Although the deviation from the right angle (at least 10°) in most cases gives a good estimate of the robustness, it is not completely reliable, since the angle is a gauge dependent property. In a different gauge, the electric transition moment is invariant, but the magnetic transition moment is not. The angle between the momenta can thus change rather widely upon a gauge transformation, even down to being zero. Only the scalar product of the two vectors, the rotational strength needs to be gauge invariant. The dimensionless ratio of the rotational and dipole strength would quantify the important concept of robustness more reliably.

APPLICATIONS

The interpretation of VCD spectra is predominantly based on computational results, as there are no reliable empirical rules to explain or predict VCD band signs or intensities. Although a number of attempts were made to formulate simple empirical or semiempirical physical models to explain at least partially the spectra, they are not in general use. Most of the heuristic models to calculate magnetic transition momenta, e.g.,[8–10] were based on such an empirical model. The only method to give a non-numeric, visual analysis of VCD intensities is the vibrational transition current density (TCD) theory[36] of Nafie. This method gives a picture of the electronic currents arising in the molecule due to nuclear vibration. The direction of flow in the vector field was interpreted to rationalize the VCD band pattern of several molecules, e.g., methyl lactate.[37] However, this rationalization is not straightforward and does not provide a simple picture, such as the ring current,[38] which is frequently invoked in nuclear magnetic resonance (NMR) spectroscopy.

Without a simple empirical interpretation of the spectra, the benefits of the continuously improving instrumentation were strongly coupled with the development of first-principles quantum chemical methods.

Configuration Determination: Performance of Methods and Basis Sets

The most important application of VCD spectroscopy is the determination of the absolute configuration of chiral organic molecules, based on the comparison of their measured and computed VCD spectra. The methodology is discussed in detail in review articles by Freedman et al.[39] and Stephens et al.,[40] presenting applications on a great variety of small to mid-sized, rigid, or conformationally flexible molecules.

The reliable determination of the absolute configuration is greatly determined by the accuracy of the calculated spectra, thus by the correct choice of the computational method (HF, MP2 or DFT, and in the latter case the type of the functional) as well as the type and size of the applied basis set.

As the VCD spectrum depends not only on the absolute configuration but on the conformation as

well, for nonrigid chiral molecules present as mixtures of conformers the calculated spectra have to be obtained as population-weighted sums of the spectra of individual structures. As a consequence, the quality of the simulated spectra is also affected by the accuracy of computational methods in determination the relative Gibbs free energies and hence the computed Boltzmann abundance of the conformers.

It is now generally accepted that the DFT methods applied to the VCD problem yield more accurate results than the HF approach, while they have about the same computational cost. Except for the smallest VCD active molecules higher electron correlation methods, including the lowest level MP2 approach, at least till the present days, were computationally too demanding, and hence were rarely used for the calculation of VCD spectra.

As an early example of comparative experimental and theoretical studies *R*-3-methylazetidin-2-one **1** and *R*-4-methylazetidin-2-one **2** were investigated by Rauk et al.[41] These calculations still relied on the VCT theory of Nafie and Freedman[11] instead of the MFP theory of Stephens.[12] The spectra of these β-lactams were recorded in CCl_4 solution at relatively high concentrations inducing the formation of hydrogen-bonded dimers. In the case of the monomers the geometry optimizations, vibrational frequency and APT calculations were performed at the HF/6–31G$^{*(0.3)}$, at the MP2/6–31G* and at the B3LYP/6–31G* levels of theory, while AATs were determined at the HF/6–31G$^{*(0.3)}$ level. For the dimers, considered large systems in the mid-1990s, the calculated VCD spectra were based on AATs obtained at the HF/6–31G level and on geometries, frequencies and APTs obtained at HF/6–31G$^{*(0.3)}$ level. The unconventional 6–31G$^{*(0.3)}$ basis set is a modified basis, in which the d orbital exponent for the C and N atoms is set to 0.3 instead of 0.8 in 6–31G*. This basis was considered to give better geometries and force fields for similar molecules.[42,43] Many bands in the measured VCD spectra could only be explained by the presence of dimers, the calculated spectra of which show surprisingly good agreement with the measured spectra as shown in Figure 1 for **1** and its H-bonded dimer $\mathbf{1}_2$ despite the use of the HF method with a modest basis set.

Later theoretical studies on halogen-substituted β-lactams [*R*-4-Hlg-azetidin-2-ones, where Hlg = F, Cl, Br] performed at much higher theoretical level (B3PW91/aug-cc-pVTZ)[44] suggested that the previous calculations on the analogous *R*-4-methylazetidin-2-one **2**[41] failed to correctly predict the sign of the carbonyl stretching vibration in the VCD spectrum, due to the use of a relatively small basis set (6–31G*). Contrary to this, Vass et al.[45] found that the sign of the carbonyl VCD band could be correctly predicted for a series of ten cyclic β-lactams even at the BPW91/6–31G** or the B3LYP/6–31G* level. Even more, the calculated VCD spectra showed an overall good agreement with the experimental ones, permitting to unambiguously assign their absolute configuration.

In order to evaluate the performance of DFT methods in the calculation of VCD spectra Stephens et al. studied a series of rigid molecules using different functionals and basis sets. The most complete study concerning the dependence of predicted VCD spectra on the choice of basis set and functional was carried out on *R*-(+)-methyloxirane **3** as test molecule.[46,47] These results are summarized in Figure 2. The spectrum of **3** was recorded in CCl_4 and compared with spectra calculated using the B3LYP functional and a series of basis sets (such as 3–21G, 6–31G*, TZ2P and cc-pVTZ, Figure 2a), as well as with spectra calculated using the cc-pVTZ basis set and different functionals (LSDA, BLYP, B3PW91, and B3LYP, Figure 2b).

From Figure 2a it is clear that the spectrum calculated with the smallest basis set (3–21G) gives poor results and a dramatic improvement is seen by increasing the size of the basis set (3–21G $\ll$ 6–31G* $<$ TZ2P $\approx$ cc-pVTZ). The two largest basis sets give very similar theoretical spectra and they are in excellent agreement with the experimental one. The moderate but widely used 6–31G* basis set combined with the B3LYP functional gives satisfactory results; however, it fails to correctly predict the sign of the weak VCD band of normal mode 8 (above 1000 cm^{-1}) and the positive band of the normal mode 10 (above 1100 cm^{-1}) is not reproduced (Figure 2a) either.

Comparison to the experimental VCD spectrum also shows that the hybrid functionals (B3LYP, B3PW91) give the best agreement with observations, while the 'pure' BLYP functional and especially the 'local' LSDA functional yields less accurate results even when used in combination with a relatively large basis set such as cc-pVTZ (Figure 2b).

Other types of oxirane derivatives such as phenyloxiranes[48] and methyl-substituted phenyloxiranes[49] were also used to benchmark the accuracy of VCD calculations. While these are not typical rigid molecules, they were shown to be single-conformer cases. (The phenyl substituent has one preferred orientation relative to the oxirane ring). Determination of the absolute configuration of 1*R*-1-methylphenyloxirane, 1*R*,2*S*-2-methylphenyloxirane and (1*R*,2*R*)-2-methylphenyloxirane was achieved by comparing their experimental VCD spectra obtained

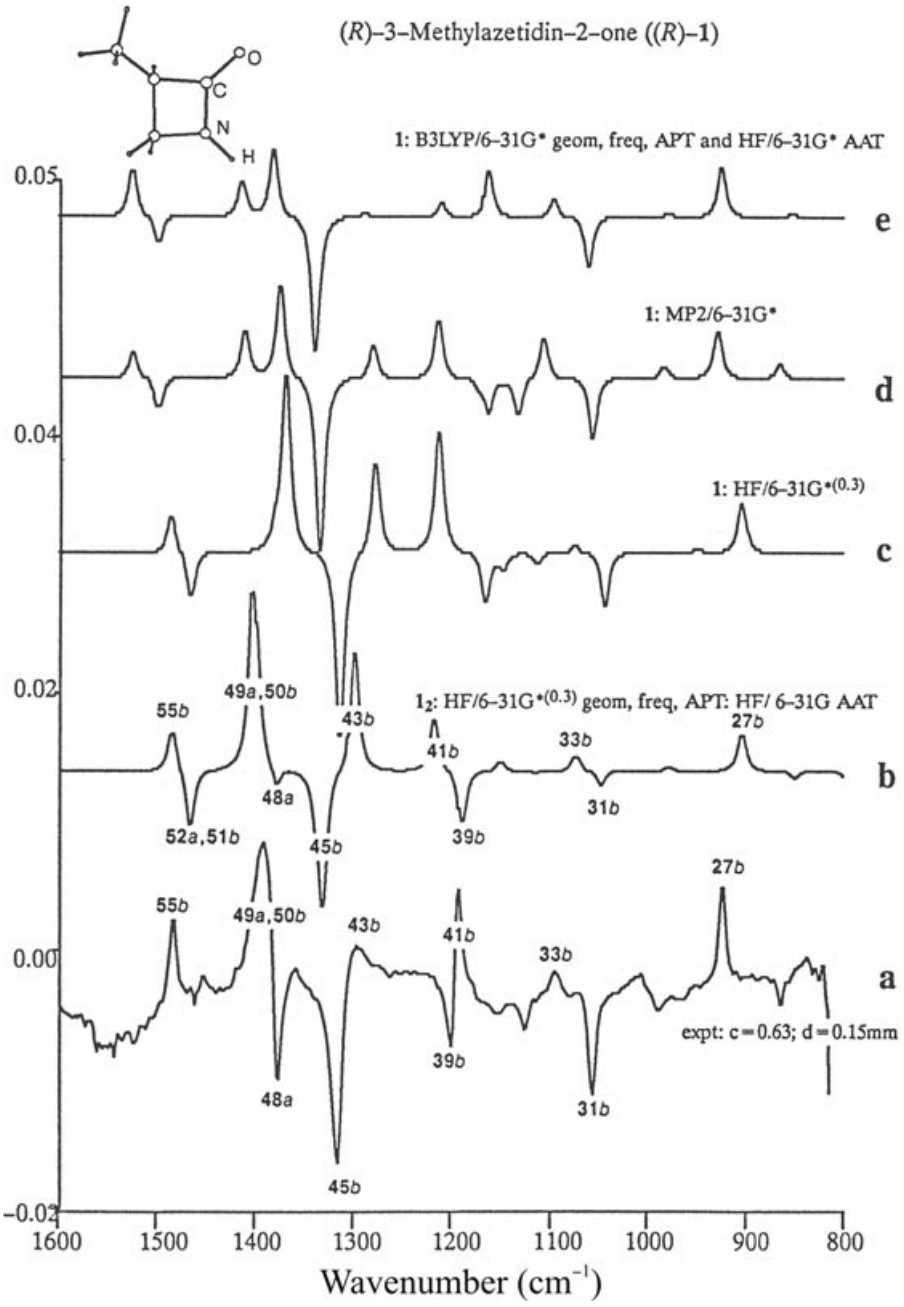

FIGURE 1 | VCD spectrum of 3*R*-(+)-methylazetidin-2-one **1** measured in CCl_4 solution (a) in comparison with the calculated spectrum of its H-bonded cyclic dimer 1_2 (b) and the calculated spectra of the monomer (c–e) obtained at different levels of theory. The calculated frequencies are scaled by 0.9 (HF) or 0.95 (MP2, B3LYP) and are simulated with a Lorentzian band shape of 10 cm^{-1} full width at half-height. (Reprinted with permission from Ref 41. Copyright 1996 Society for Applied Spectroscopy.)

as neat liquid films or CCl_4 solutions with the spectra calculated at the B3LYP/aug-cc-pVTZ level, however, results obtained with smaller basis sets such as 6–31++G** and aug-cc-pVDZ were also presented.[49] An overall good agreement between the 6–31++G** and the aug-cc-pVTZ basis sets was observed, while the aug-cc-pVDZ basis set often yielded markedly different results.

Stephens et al.[40,50] demonstrated that TZ2P represents a good compromise between accuracy and the size of the basis set, when used in combination with the B3LYP or B3PW91 functionals. A recent study[50] on the chiral alkane *S*-(+)-D_3-anti-*trans*-anti-*trans*-anti-*trans*-perhydrophenylene **4** (Figure 3) clearly shows the efficiency of this basis set in correctly predicting the frequency and rotatory strength

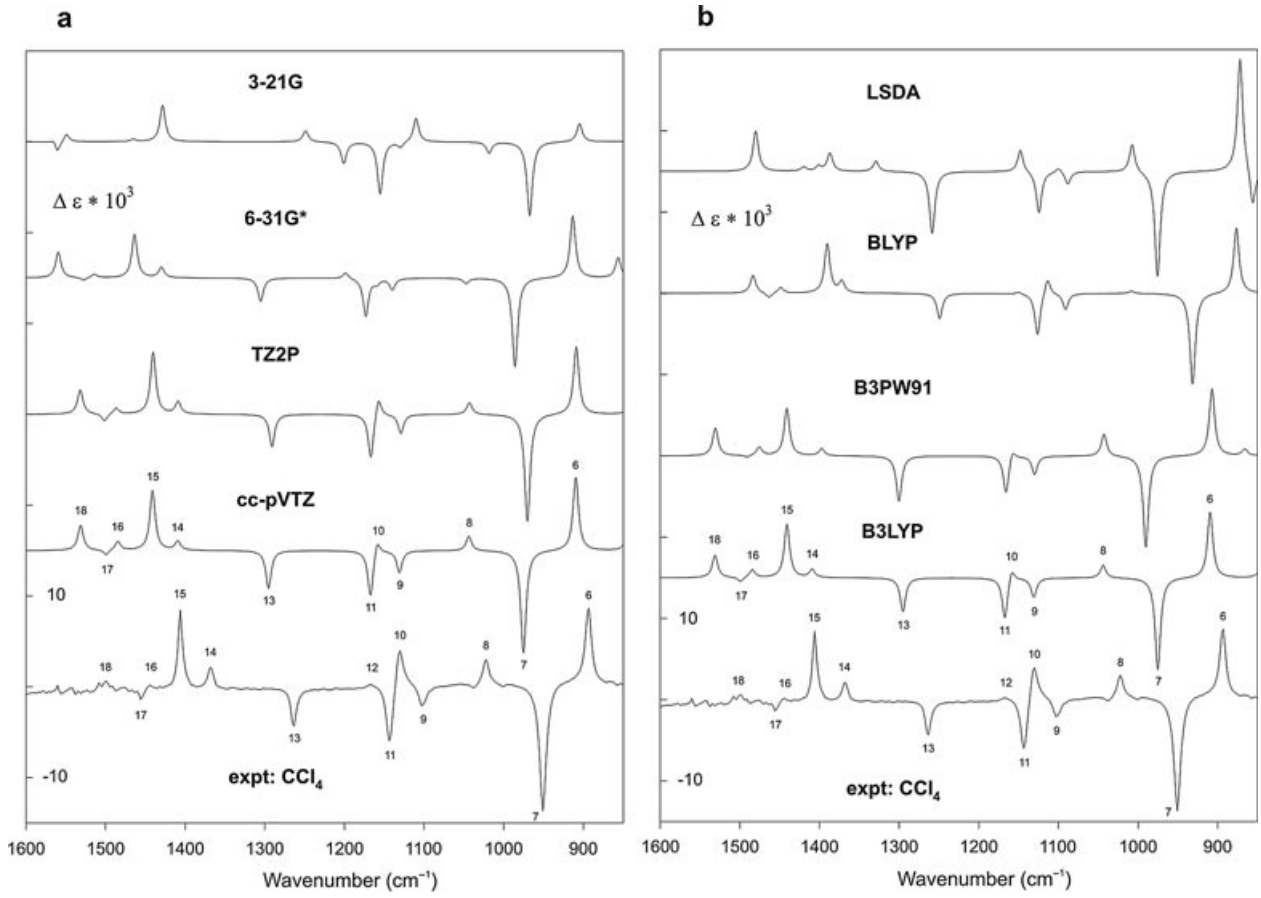

FIGURE 2 | Mid-IR VCD spectrum of *R*-(+)-methyloxirane recorded in CCl_4 solution in comparison with calculated spectra using the B3LYP functional with a range of basis sets (a) and the cc-pVTZ basis set with a range of functionals (b). Band shapes are Lorentzian with 4 cm^{-1} full width at half-height. Fundamentals are numbered. (Reprinted with permission from Ref 46. Copyright 2002 American Chemical Society.)

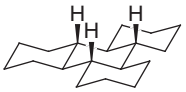

4

FIGURE 3 | Structure of *S*-(+)-D_3-anti-*trans*-anti-*trans*-anti-*trans*-perhydrophenylene **4**.

values (see Figure 4). The spectra calculated with the B3PW91 functional proved to be slightly more accurate than those obtained with the B3LYP functional. The paper also provides comparative results obtained with B3PW91/TZ2P, B3PW91/6–31G*, and HF/TZ2P calculations summarized in Table 1, showing that the accuracy of methods in predicting the rotational strength values decreases in the order of B3PW91/TZ2P > B3PW91/6–31G* > HF/TZ2P. The last parameter in Table 1, termed relative scatter ratio, provides a quantitative measure of the increase in scatter from the 'line of perfect agreement' of the data points in the plot of calculated versus experimental rotational strengths over the scatter of the B3PW91/TZ2P data.

There are also examples in the literature on chiral transition metal complexes, where the correct choice of the basis set for the calculation of their VCD spectra is not always trivial. Stephens et al.[51] confirmed the absolute configuration of the enantiomeric tricarbonyl-η^6-N-pivaloyltetrahydroquinoline-chromium(0) **5** (Figure 5) by VCD spectroscopy, where the chiral heteroaromatic ligand is attached to the Cr(0) atom by π interaction.[51] A careful conformational analysis showed that the complex is present as a mixture of 11 conformers. Out of the conformers the lowest-energy one is predominant, thus mainly determining the spectral features. VCD spectra were calculated using the functionals and basis sets listed in Table 2. It was found that the calculated spectrum varied

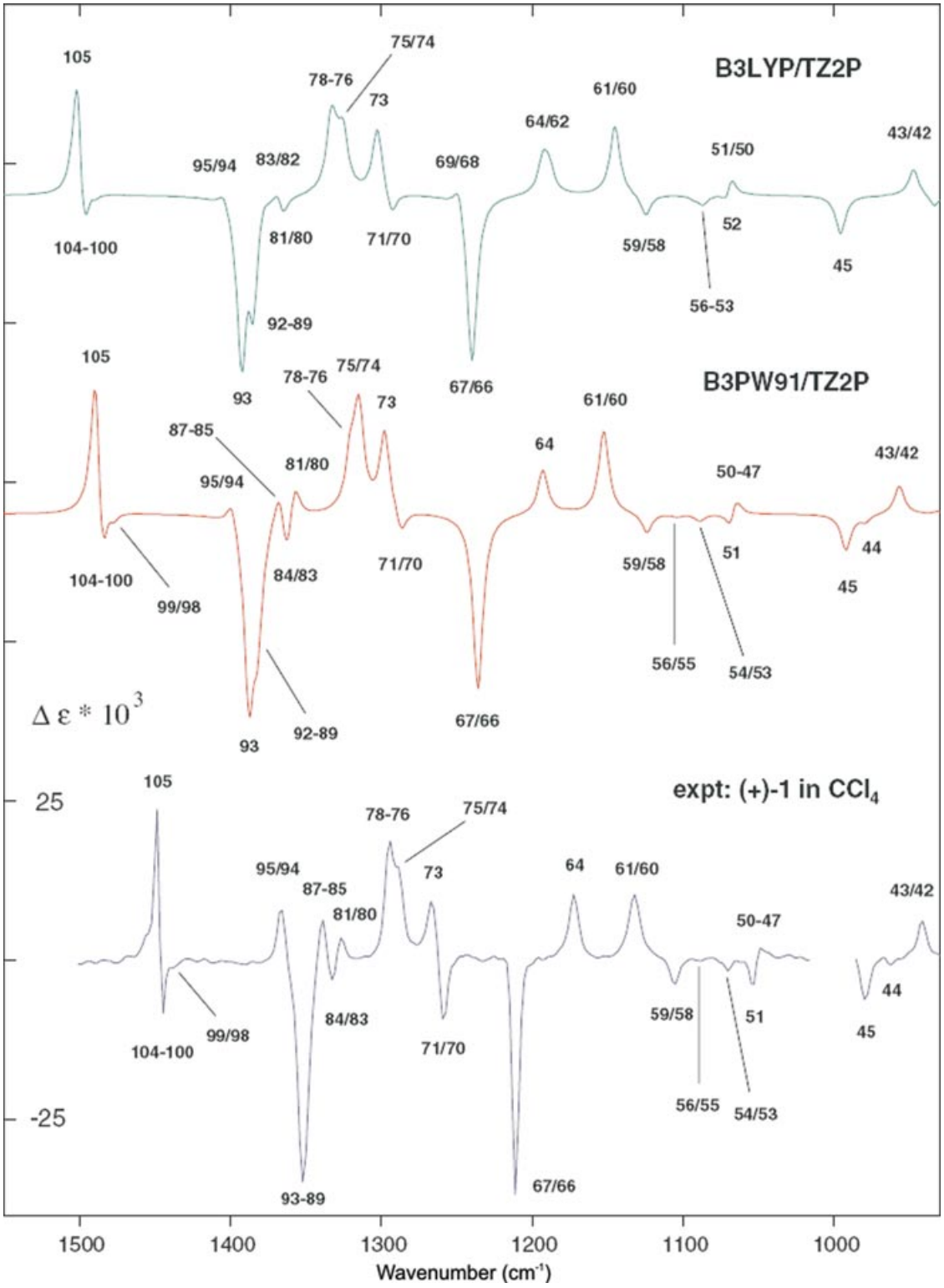

FIGURE 4 | Comparison of the B3LYP/TZ2P, B3PW91/TZ2P and experimental VCD spectra of **4**. The bandshapes of the calculated spectra are Lorentzian with 4 cm^{-1} full width at half-height. The numbers define the fundamental modes of **4** contributing to the spectral bands. (Reprinted with permission from Ref 50. Copyright 2007 Springer.)

TABLE 1 | The Accuracies of the Calculated Rotational Strengths of *S*-(+)-D_3-anti-*trans*-anti-*trans*-anti-*trans*-Perhydrophenylene **4**

Calculation Method	Mean Absolute Deviation[1]	RMS Deviation[2]	Relative Scatter Ratio[3]
B3PW91/TZ2P	7.5405	9.8555	1.0000
B3PW91/6–31G*	9.3879	14.1712	1.6078
HF/TZ2P	11.0170	16.4465	2.5656

Reprinted with permission from Ref 50. Copyright 2007 Springer.
[1]Average of the absolute deviations of calculated rotational strengths from the experimental rotational strengths.
[2]RMS deviation of calculated and experimental rotational strengths.
[3]The average of the ratios of absolute deviations of calculated and experimental rotational strengths for the method used in the calculation to the absolute deviations for the B3PW91/TZ2P method.

TABLE 2 | The Accuracies of the Calculated Rotational Strengths of *S*-(+)-**5** as a Function of Functional and Basis Set

Calculation Method	Mean Absolute Deviation[1]	RMS Deviation[2]	Relative Scatter Ratio[3]
B3PW91/6–311++G(2d,2p)	12.8396	21.7985	1.0000
B3PW91/TZVP	13.5441	22.9008	1.2502
B3PW91/6–31G*	19.0004	29.5905	3.1804
B3LYP/6–311++G(2d,2p)	24.1768	38.6040	4.0217
B3LYP/TZVP	23.7171	39.6895	3.6407
B3LYP/6–31G*	24.2667	34.3545	5.1522

Reprinted with permission from Ref 51. Copyright 2008 Elsevier Science.
[1]Average of the absolute deviations of calculated rotational strengths from the experimental rotational strengths.
[2]RMS deviation of calculated and experimental rotational strengths.
[3]The average of the ratios of absolute deviations of calculated and experimental rotational strengths for the method used in the calculation to the absolute deviations for the B3PW91/6–311++G(2d,2p)method.

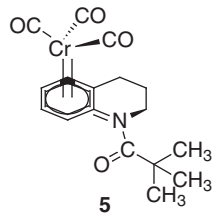

5

FIGURE 5 | Structure of *S*-(+)-tricarbonyl-η^6-N-pivaloyl-tetrahydroquinoline-chromium(0) **5**.

significantly as the basis set was increased in size from 6–31G*. The basis sets TZVP and 6–311++G(2d,2p) gave similar spectra demonstrating that both are reasonably good approximations to the complete basis set limit. The results obtained by these latter basis sets are also in excellent agreement with the experimental spectrum (see Figure 6). Since neither of these basis sets are defined for the elements of the fifth to seventh periods, and relativistic effects should also be taken into account for these heavy elements, one has to make compromises in calculating the spectra of several transition metal complexes.

For transition metal complexes the LanL2DZ basis was also suggested[52,53] which includes Dunning/Huzinaga full double-ζ basis on the first row elements, and the Los Alamos effective core potential (ECP) plus double-ζ basis on Na–Bi. Nafie et al.[52] successfully used the LanL2DZ as well as the 6–31G(d)[C, H, N]/Stuttgart ECP [Co] in combination with the B3LYP functional for predicting the distribution of conformers and calculating the VCD spectrum of the chiral (+)-tris(ethylenediaminato)cobalt(III) complex.

Sato et al.[53] studied the VCD spectra of a series of [M(III)(acac)$_3$] (acac = acetylacetonato; M = Cr, Co, Ru, Rh, Ir, and Al) **6** and [M(III)(acac)$_2$(dbm)] (dbm = dibenzoylmethanato; M = Cr, Co, and Ru) **7** (Figure 7) complexes experimentally and theoretically in order to see the effect of the central metal ion on the vibrational dynamics of ligands. As in the case of the previously mentioned tris(ethylenediaminato)cobalt(III) complex, optical activity appears as a result of the chiral arrangement of inherently achiral ligands around the metal atom. The two enantiomeric forms are termed as Δ and Λ. The calculations were performed for the Δ

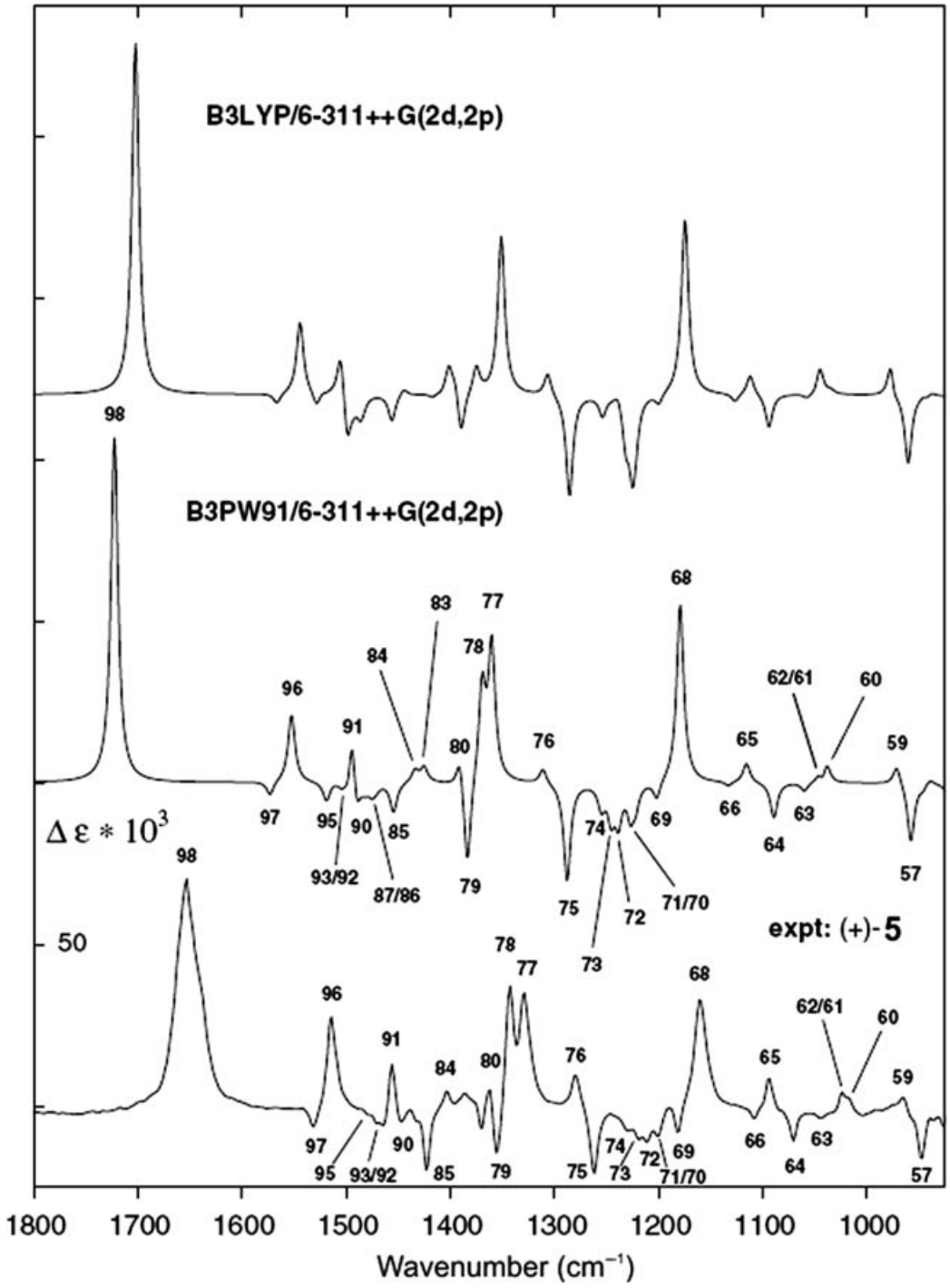

FIGURE 6 | Comparison of the B3PW91/6–311++G(2d,2p) and B3LYP/6–311++G(2d,2p) VCD spectra of the lowest-energy conformer of *S*-**5** to the experimental VCD spectrum of (+)-**5**. Band shapes are Lorentzian with 4 cm^{-1} full width at half-height. The numbers are those of the fundamentals. (Reprinted with permission from Ref 51. Copyright 2008 Elsevier.)

enantiomers of **6** and **7** using the B3LYP functional in combination with the LanL2DZ basis set for the metal atom and 6–31G* for C,H,O. For certain coupled C–O stretching modes in the 1500 to 1300 cm^{-1} spectral region the theoretical results proved to be sufficiently dependable to assign the VCD bands.

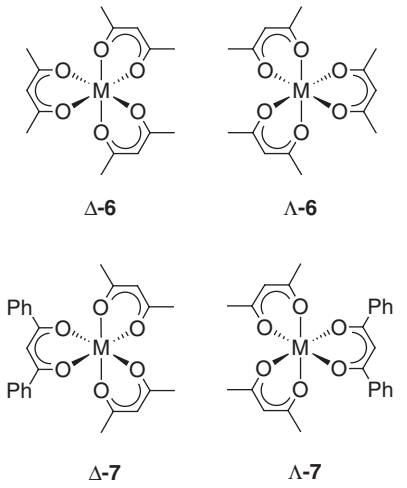

FIGURE 7 | Structure of Δ and Λ enantiomers of metal complexes $[M(III)(acac)_3]$ (acac = acetylacetonato; M = Cr, Co, Ru, Rh, Ir, and Al) **6** and $[M(III)(acac)_2(dbm)]$ (dbm = dibenzoylmethanato; M = Cr, Co, and Ru) **7**.

Conformational Studies of Biomolecules

As it is shown above VCD spectroscopy combined with calculations has been extensively used for the determination of absolute configuration and the 'absolute conformation' (i.e., simultaneous configuration and configuration determination) of a large variety of conformationally flexible chiral molecules. In the case of biomolecules such as carbohydrates, nucleotides, peptides, or proteins the absolute configuration of the building blocks is usually known and VCD is primarily used for the determination of their conformation.

Taniguchi and Monde have performed a systematic measurement on carbohydrates.[54] They have found that the intense VCD peak around 1145 cm^{-1} is characteristic for axial glycosidic sugars. It was found that the sign of this 'glycoside band' reflects not only the anomeric configuration but also the pyranose conformation. In good correspondence with the systematic experimental findings (see Figure 8), B3LYP/6–31G** calculations also supported these results.

The interpretation of VCD spectra of nucleotides is more challenging. As an example Bouř et al.[55] investigated the structure of deoxyoctanucleotides by IR, VCD spectroscopy combined with theoretical calculations. Since for these large systems, containing about 1000 atoms, complete DFT calculations are not possible, they developed a method, called

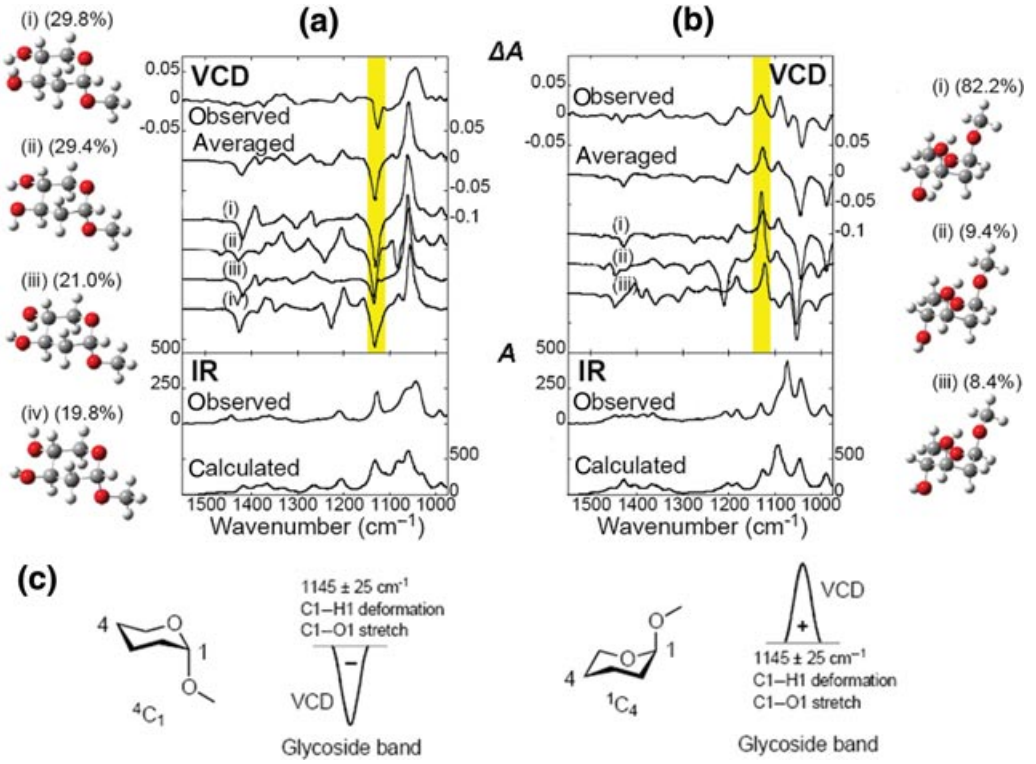

FIGURE 8 | Experimental and calculated VCD spectra of a) 2-deoxy-α-D-xylopyranoside ($CDCl_3$, 0.10 M, 100 μm CaF_2 cell) and b) 2-deoxy-β-D-xylopyranoside ($CDCl_3$, 0.10 M, 100 μm CaF_2 cell). The theoretical spectra were obtained from the computed spectra of the individual conformers at the B3LYP/6–31G** level of theory by weighted averaging using the Boltzmann populations shown in parentheses. The glycoside band is shaded in the Figure. Conclusions on the VCD sign of the glycoside band are shown on panel c). (Reprinted with permission from Ref 54. Copyright 2007 Wiley-VCH.)

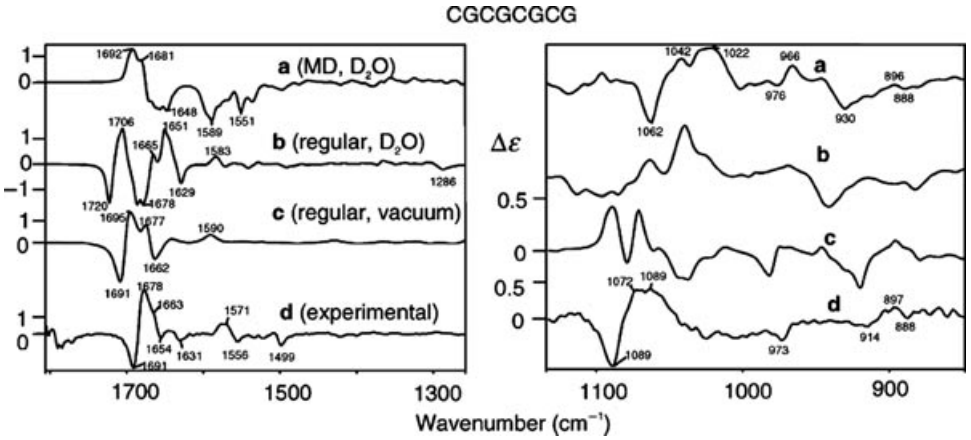

FIGURE 9 | VCD spectra of the d(CGCGCGCG) octanucleotide simulated for the MD (a) and regular X-ray geometry with (b) and without (c) the solvent, as compared to the experimental spectrum (d). The base (left) and sugar-phosphate (right) vibration regions are expanded separately. (Reprinted with permission from Ref 55. Copyright 2005 American Chemical Society.)

'Transfer of Molecular Property Tensors' for computing VCD spectra of large molecular systems.[56] In this case, they first obtained an averaged structure of the hydrated model compounds from molecular dynamics simulations using the AMBER force field. Then the model compounds were divided into 24 fragments with approximately equal size. For these fragments the force constants and molecular property tensors (APT and AAT) were calculated at the BPW91/6–31G** level with or without considering the effect of the solvent (water). Then these frequencies and tensors were transferred to the original molecules (with molecular dynamics (MD) based averaged or X-ray-based geometries). Figure 9 shows the results obtained for the d(CGCGCGCG) octanucleotide. In this particular case, the simulated spectrum for the average MD structures (trace a) agrees reasonably with the experiment (trace d) in the lower wave number region (with more contributions from the sugar and phosphate moieties), while in the higher wave number part (reflecting more from the contribution of the bases), the X-ray-based structures (traces b and c) gave better agreement.

Of the different classes of biomolecules, peptides and proteins are the most extensively studied by VCD spectroscopy, hence we present a more detailed summary of work on these systems. The most characteristic and intense vibration of peptides and proteins in the IR and VCD spectra is the amide I mode (termed amide I′ in D_2O solution due to deuteration of amide groups), consisting of ~80% C=O stretch.[57] Other vibrational modes of the amide group such as amide II (mostly in-plane N–H bending + some C–N stretch contribution) as well as amide III (mostly C–N stretch + some N–H in-plane bending with contribution from δ C_α–H of the α-methyne group) may also give useful information about the conformation.[58–60] The amide III mode has weak IR and VCD bands, it can be examined better by Raman Optical Activity (ROA) spectroscopy.[61]

The band shape of the amide I–II spectral region (1700–1500 cm^{-1}) is determined by (1) the local conformation of the amino acid residue characterized by the φ and ψ dihedral angles, (2) coupling of amide I vibrational modes of neighboring amide groups and (3) frequency shifts due to different types of H-bonding schemes, which explains the sensitivity of VCD on the secondary structural elements of polypeptides and proteins.

From a large number of analyzed experimental VCD spectra and structural information derived from alternative methods (ECD, NMR, X-ray crystallography) rudimentary empirical rules were formulated for predicting the shape of amide I–II VCD bands, especially for periodic secondary structures like helices and sheets. Right-handed α-helical and 3_{10}-helical structures were found to be characterized by a positive amide I VCD couplet (pair of bands of opposite sign with the positive component at lower frequency) centered at ~1650 cm^{-1} with negative amide II. The main difference between the VCD spectra of these structures is the ratio of the amide I and II intensities. Left-handed helices such as the polyproline II (PPII) conformation and the so-called 'unordered' secondary structures are characterized by a negative amide I couplet (pair of bands of opposite sign with the negative component at lower frequency). Finally, β-sheets often give a weak negative amide I band (around 1630 cm^{-1}) or a negative couplet. The VCD band intensities and patterns of β-sheets show a much greater variation then those of helical structures.[62]

The first attempts to predict the rotational strengths of amide I modes of typical polypeptide secondary structures by calculations relied on the coupled oscillator model (see, e.g., Ref 63), which, by crudely estimating the transition magnetic moment, treated the sequence of vibrating amide groups as a system of coupled oscillating electric dipoles. This simple model could only lead to so-called conservative VCD spectra (couplets with negative and positive side-lobes of equal intensity), which was suitable for predicting the bisignate (couplet) character of the amide I VCD-band of α-helices but failed for the single-signed (or predominantly negative) amide II band. The situation was even worse in the case of β-sheet structures. Later the coupled oscillator model was abandoned in favor of the more accurate DFT/MFP/GIAO method, with the only limiting factor being the size of the studied polypeptide molecules.

For larger oligo- and polypeptides with a periodic structure (helices, sheets, strands) the abovementioned 'Transfer of Molecular Property Tensors' approach [56] can be applied. This method was used for modeling VCD spectra of α-helical,[64–67] 3_{10}-helical,[68] PPII,[67] β-sheet,[69] and β-hairpin[70,71] structures with a great deal of success. In these calculations mostly the 'pure' (nonhybrid) BPW91 functional was used (with the 6–31G** or sometimes the 6–31G* basis set), which, in the case of a number of structures, was found to give better results for the rotational strengths of the amide I and II modes. (This may not always be the case for lower frequency modes, which are less important for the vibrational spectroscopy of peptides.) Furthermore, it is much more economical for force field computation than hybrid functionals (e.g., B3LYP) commonly used for vibrational analyses.

One of the great successes of VCD spectroscopy is the discrimination of α- and 3_{10}-helical structures based on the intensity ratio of the amide I and amide II VCD bands. The positive amide I couplet of α-helical peptides is more intense than the negative amide II band, while for 3_{10}-helical peptides the opposite is true. (Furthermore, the amide I couplet of 3_{10}-helical peptides is weaker). The 3_{10}-helical conformation is stabilized by incorporation of α-disubstituted amino acid residues such as α-aminoisobutyric acid (Aib) in the sequence. Based on computational studies on well-chosen model peptides with or without Aib residues such as Ac-$(Ala)_n$-NH_2, Ac-$(Aib\text{-}Ala)_n$-NH_2, and Ac-$(Aib)_n$-NH_2 Keiderling et al.[68] theoretically confirmed the validity of the above observations. Complete BPW91/6–31G** calculations were carried out for shorter models, with up to 6 amino acid residues, constrained in α-helical or 3_{10}-helical conformations. For larger models with 12 amino acid residues the method involving the transfer of molecular property tensors from the shorter models molecules was applied. Although in the case of 3_{10}-helical peptides the change in Aib content had a higher influence on amide I band intensities than in the case α-helical peptides, the basic pattern of amide I and II relative intensities of the two different helical structures was different enough to be distinguished (Figure 10).

In addition to the different helices and β-sheets, the third group of ordered (regular) secondary structures of proteins includes the turns, out of which β-turns (β-bends, reverse turns) are the most abundant and best-characterized. They comprise four amino acid residues connected by three amide groups and may be stabilized by $1\leftarrow4$ (C_{10}) intramolecular H-bonding (IHB). The other important type of turns are γ-turns, containing only three amino acid residues, being stabilized by with $1\leftarrow3$ (C_7) IHB (for the classification of turns see, e.g., Refs 72 and 73). The vibrational spectroscopy of different turns has been reviewed by Vass et al.,[73] covering the literature before 2002. At that time only a few VCD studies on turns supported by quantum chemical calculations were available.

Spectroscopic characteristics of turns can be studied on small linear and cyclic model peptides which cannot form large sequences of periodic secondary structures such as helices and turns. Nevertheless, until recently only a few reliable VCD data were published in the field. The available studies mostly relate to β-turns.

Calculations on β-hairpin model peptides, in which chain-reversals occur via β-turn structures, revealed that type I′ β-turns (mirror image of the most common type I β-turns) with D-Pro–Gly sequence in the corner positions give a negative amide I VCD couplet[70] but the band shape changed with the size and type (open-chain or cyclic) of the model. Besides the isolated model compound, simulations were carried out also on the solvated molecule by an explicit solvent model (see below).

Lovas et al.[74] studied the VCD spectra of disulfide bridged Ac–Cys–Xxx–Yyy–Cys–NH_2 cyclic tetrapeptides, where Xxx and Yyy are amino acids which were previously found to occur in different types of β-turns preferentially. The calculations were carried out at the B3LYP/6–31G* level for the isolated molecules in vacuum. Model peptides with Pro–Gly or Pro–D-Ala in corner positions were suggested to adopt a type II, while Pro-Asn and Pro-Ser models a type VIII β-turn conformation.

A recent theoretical paper by Keiderling et al.[75] presents a systematic analysis of the expected amide

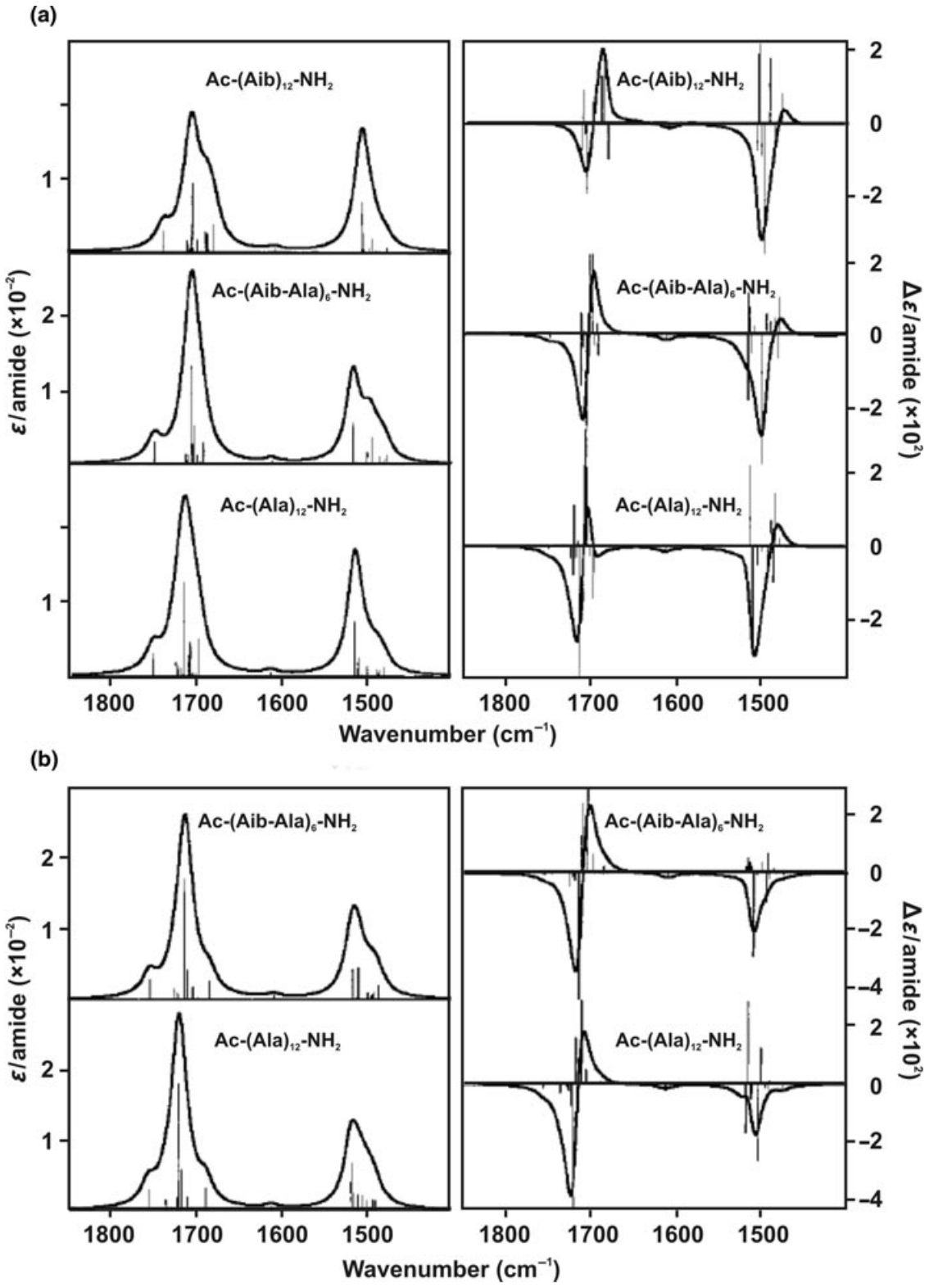

FIGURE 10 | Simulated IR (left) and VCD (right) spectra of model dodecapeptides with (a) 3_{10}-helical or (b) α-helical structure. (Reprinted with permission from Ref 68. Copyright 2002 American Chemical Society.)

I and II VCD band patterns associated with standard (types I–III) and mirror-image (types I′–III′) β-turn structures. Calculations were performed at the BPW91/6–31G** level on Ac–Xxx–Yyy–NHMe type model peptides with different amino acids in the corner positions. Calculations were carried out on different types of turns neglecting and considering the effect of solvent while using either standard geometries or using fully optimized structures. It was shown that type I and III β-turns have a very similar pattern (positive couplet in the amide I), making their discrimination quite difficult. One important conclusion is that in the case of type II turns, the key is not the amide I mode, but the amide II which tends to give an opposite sign pattern, allowing their discrimination from type I (or III) turns.

Solvent Effects and Chirality Transfer

Although there are a few VCD studies in the gas phase[76,77] or in low-temperature inert matrices,[78–83] where the intermolecular interactions are minimized, most VCD studies, including the ones on peptides and proteins are carried out either in their native matrix, i.e., in aqueous (often D_2O) solution or in organic (usually deuterated) solvents suitable for IR measurements. Therefore it is important to briefly discuss both the possible effects of the interaction with the solvent on the VCD spectra and the computational armamentarium which can take these effects into account.

Solvation can change the geometry of conformers, can alter or even drastically change their relative abundance, and can directly affect the VCD spectra by perturbing the electronic and magnetic properties. Baerends et al.[84] have distinguished and studied six cases of effects of solvent-solute interactions: (1) no or small change in rotational strengths of a solute's vibrational modes, (2) a change in sign; (3) a change in magnitude; (4) nonzero rotational strengths appearing for a vibrational mode of the interacting achiral solvent molecule (so-called 'induced chirality' or 'chirality transfer'); (5) large frequency shifts with simultaneous giant enhancement of the IR and VCD intensities; (6) emergence of new peaks.

The most direct way of considering the effect of solvent is to perform calculations on the system of solvated peptide surrounded by an explicitly modeled solvent, e.g., molecules (see Figure 11a). Although in this case spectral effects arising from specific interactions can be evaluated, it is the most computationally demanding method since a sufficiently high number of solvent molecules and several possible spatial orientations have to be considered. As a consequence of this, this method cannot be efficiently used for larger molecular systems, the examples of such calculations in the literature[75,85] deal with smaller or conformational space restricted peptides.

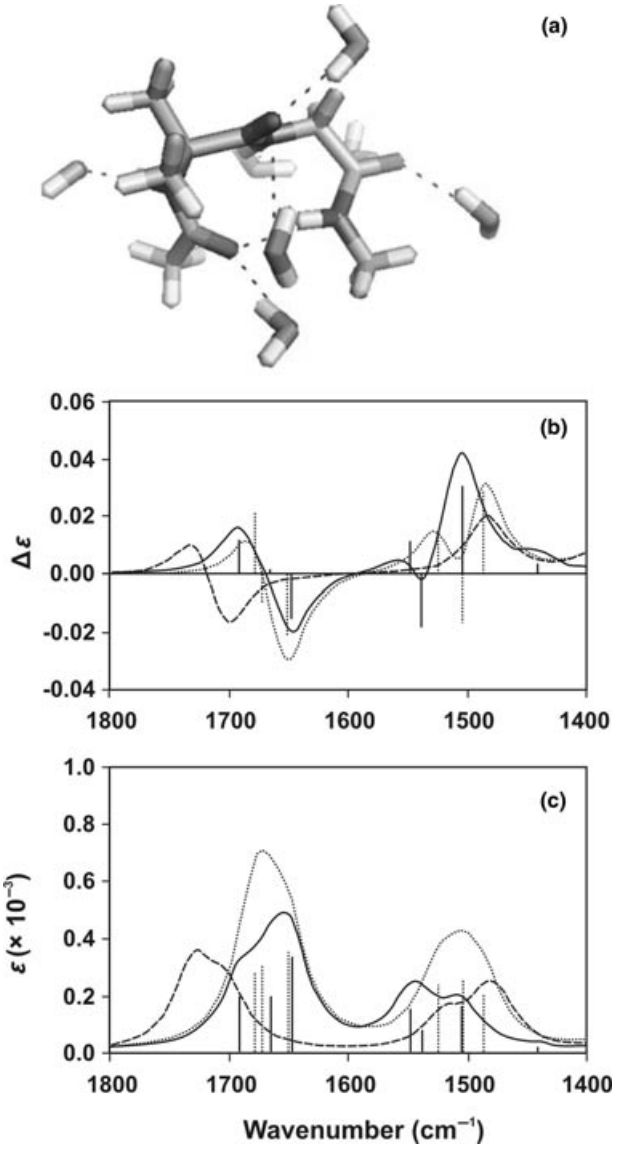

FIGURE 11 | The effect of solvent model on the simulated amide I-II VCD (b) and IR (c) absorption bands of model peptide Ac-Aib-Gly-NHMe forming a type I′ β-turn, computed at the BPW91/6–31G** level. The spectra were simulated for the optimized minimal hydration structure shown in (a) with seven explicit water molecules (solid line), for the COSMO solvent model (dotted) and for vacuum (dashed). (Reprinted with permission from Ref 75. Copyright 2008 Springer.)

Less rigorous computations accounting for solvent effects apply the polarizable continuum (PCM, IEF-PCM) or conductor-like screening (CPCM, COSMO) solvent models which are available for VCD calculation in quantum chemical software

packages like Gaussian. Out of polarizable continuum models the variant based on the integral formalism (IEF-PCM)[86–88] is the most popular, with prebuilt parameters for a large number of solvents. For a detailed discussion of different types of quantum mechanical continuum solvation models (including PCM and COSMO) see the review article of Tomasi et al.[89]

As an example, the effect of solvent on the amide I-II VCD and IR absorption bands of a type I′ β-turn forming model peptide Ac-Aib-Gly-NHMe was theoretically investigated.[75] The experimentally observable gap between the amide I and II bands is highly overestimated when the isolated model compound is calculated in the vacuum. This can considerably be improved by employing the COSMO model, while an even better result was obtained by explicitly considering the solvent molecules. Furthermore, some changes in the relative intensities of component bands, especially in the amide II region, were observed, but the main characteristic of a type I′ β-turn, i.e., the negative amide I VCD couplet was not altered when the solvent effects were taken into account. See Figure 11.

There are few theoretical and experimental studies on the above-mentioned chirality transfer phenomenon.[80,84,90–99] Recent reviews by Zehnacker and Suhm,[100] as well as by Sadlej et al.[101] summarize the developments in this field. Here we emphasize the fact that although in many cases both the computations and the experimental observations resulted in considerably large induced rotational strengths for the vibrational mode of the interacting achiral solvent molecule, the computations and observations (i.e., intensities and signs) were coinciding poorly. It was computationally demonstrated that small deviations of the intermolecular torsional coordinates from the equilibrium structure can result in significant intensity and sign changes of the complexation induced VCD band.[83] Baerends et al.[99] interpreted this finding by taking the following into consideration. In isolated achiral molecules the electric and magnetic transition dipole vectors would be perpendicular to each other. The weak complexation with a chiral molecule perturbs only slightly these two vectors; hence each vibrational mode of the complexed achiral molecule should have small, easily perturbed (non-robust) rotational strengths.

Finally, it is worth mentioning that there are studies in the literature, in which the effect of external parameters, such as the pH or the temperature on VCD spectra are systematically investigated. As an example, Nafie et al.[102] investigated the pH-induced spectral changes in L-alanine by two-dimensional VCD correlation spectroscopy (COS). They have demonstrated that this method is a useful tool that provides enhanced chemical information over traditional one-dimensional spectra, and it can aid the spectrum assignments based on comparison with theoretical calculations.

CONCLUSION

The theoretical evaluation of VCD spectra became a workhorse application of quantum chemistry in the last decade. The comparison of computed and measured VCD spectra gives a very useful tool in the hands of chemists interested in determining absolute configurations or studying the conformational landscape of molecules. The aim of computational chemists now should be to explore and delineate the limitations of the proven theory (GIAO/DFT/MFP) used in the calculations in order to make their application reliable for everyday use. In particular, the effects of electronic correlation, vibrational anharmonicity or unpaired electrons are neglected or only partially implemented in currently available approaches. The effect of low-energy excited states on calculated VCD spectra should also be explored further.

The rotational strengths of many vibrational modes are sensitive to the molecular environment. Therefore both the experimental techniques in which the intermolecular interactions are minimized, and the theoretical approaches which simulate the solvent effects have to be further developed. Intrinsic reliability tests, similar to the robustness concept, are also needed for future applications. The full automatization of computational procedures including conformational mapping, reliability tests, inclusion of necessary empirical corrections, graphical interfaces, and implementation of semi-automatic spectrum assignments could make VCD spectroscopy the most powerful, primary absolute configuration determination tool not only for fundamental, but also for applied, e.g., pharmaceutical, research.

ACKNOWLEDGEMENT

The authors acknowledge support of this work by the Hungarian Scientific Research Fund (OTKA K75877 and K81175).

REFERENCES

1. Rosenfeld L. Quantenmechanische Theorie der natürlichen optischen Aktivität von Flüssigkeiten und Gasen. *Z Physik* 1929, 52:161–174. doi:10.1007/BF01342393
2. Warnke I, Furche F. Circular dichroism:eletronic. *WIREs Comput Mol Sci* 2011. In press.
3. Holzwarth G, Hsu EC, Mosher HS, Faulkner TR, Moscowitz A. Infrared circular dichroism of carbon-hydrogen and carbon-deuterium stretching modes. Observations. *J Am Chem Soc* 1974, 96:251–252. doi:10.1021/ja00808a042
4. Nafie LA, Cheng JC, Stephens PJ. Vibrational circular dichroism of 2,2,2-trifluoro-1-phenylethanol. *J Am Chem Soc* 1975, 97:3842–3843. doi:10.1021/ja00846a061
5. Nafie LA, Keiderling TA, Stephens PJ. Vibrational circular dichroism. *J Am Chem Soc* 1976, 98:2715–2723. doi:10.1021/ja00426a007
6. Person WB, Newton JH. Dipole moment derivatives and infrared intensities. I. Polar tensors. *J Chem Phys* 1974, 61:1040–1049. doi:10.1063/1.1681972
7. Mead CA, Moscowitz A. Dipole length versus dipole velocity in the calculation of infrared intensities with Born–Oppenheimer wave functions. *Int J Quantum Chem* 1967, 1:243–249. doi:10.1002/qua.560010304
8. Holzwarth G, Chabay I. Optical activity of vibrational transitions: a coupled oscillator model. *J Chem Phys* 1972, 57:1632–1635. doi:10.1063/1.1678447
9. Schellman JA. Vibrational optical activity. *J Chem Phys* 1973, 58:2882–2886. doi:10.1063/1.1679592
10. Nafie LA, Walnut TH. Vibrational circular dichroism theory: a localized molecular orbital model. *Chem Phys Lett* 1977, 49:441–446. doi:10.1016/0009–2614(77)87010–3
11. Nafie LA, Freedman TB. Vibronic coupling theory of infrared vibrational transitions. *J Chem Phys* 1983, 78:7108–7116. doi:10.1063/1.444741
12. Stephens PJ. Theory of vibrational circular dichroism. *J Phys Chem* 1985, 89:748–752. doi:10.1021/j100251a006
13. Buckingham AD, Fowler PW, Galwas PA. Velocity-dependent property surfaces and the theory of vibrational circular dichroism. *Chem Phys* 1987, 112:1–14.
14. Nafie LA. Adiabatic molecular properties beyond the Born-Oppenheimer approximation. Complete adiabatic wave functions and vibrationally induced electronic current density. *J Chem Phys* 1983, 79:4950–4957. doi:10.1063/1.445588
15. Stephens PJ. Gauge dependence of vibrational magnetic dipole transition moments and rotational strengths. *J Phys Chem* 1987, 91:1712–1715. doi:10.1021/j100291a009
16. Nafie LA. Velocity-gauge formalism in the theory of vibrational circular dichroism and infrared absorption. *J Chem Phys* 1992, 96:5687–5702. doi:10.1063/1.462668
17. Jalkanen KJ, Kawiecki RW, Stephens PJ, Amos RD. Basis set and gauge dependence of ab initio calculations of vibrational rotational strengths. *J Phys Chem* 1990, 94:7040–7055. doi:10.1021/j100381a023
18. Hansen AE, Bouman TD. Localized orbital/local origin method for calculation and analysis of NMR shieldings. Applications to ^{13}C shielding tensors. *J Chem Phys* 1985, 82:5035–5047. doi:10.1063/1.448625
19. Bak KL, Hansen AE, Stephens PJ. Ab initio calculations of atomic polar and axial tensors using the localized orbital/local origin (LORG) approach. *J Phys Chem* 1995, 99:17359–17363. doi:10.1021/j100048a009
20. Ditchfield R. Self-consistent perturbation theory of diamagnetism. *Mol Phys* 1974, 27:789–807. doi:10.1080/00268977400100711
21. London F. Theorie quantique des courants interatomiques dans les combinaisons aromatiques. *J Phys Radium* 1937, 8:397–409. doi:10.1051/jphysrad:01937008010039700
22. Frisch MJ, Trucks GW, Schlegel HB, Scuseria GE, Robb MA, Cheeseman JR, Montgomery J, Vreven T, Kudin KN, Burant JC, et al. *Gaussian 03, Gaussian, Inc.*, Wallingford, CT. 2004.
23. Stephens P, Ashvar C, Devlin F, Cheeseman J, Frisch M. Ab initio calculation of atomic axial tensors and vibrational rotational strengths using density functional theory. *Mol Phys* 1996, 89:579–594. doi:10.1080/00268979609482495
24. DALTON, a molecular electronic structure program, Release 2.0, see http://www.kjemi.uio.no/software/dalton/dalton.html. 2005.
25. Bak KL, Jorgensen P, Helgaker T, Ruud K, Jensen HJA. Gauge-origin independent multiconfigurational self-consistent-field theory for vibrational circular dichroism. *J Chem Phys* 1993, 98:8873–8887. doi:10.1063/1.464445
26. Nicu VP, Neugebauer J, Wolff SK, Baerends EJ. A vibrational circular dichroism implementation within a Slater-type-orbital based density functional framework and its application to hexa- and hepta-helicenes. *Theor Chem Acc* 2007, 119:245–263. doi:10.1007/s00214–006-0234-x
27. PQS version 3.2, Parallel Quantum Solutions, 2013 Green Acres road, Fayetteville, Arkansas 72703. 2006.
28. Amos RD, Handy NC, Jalkanen KJ, Stephens PJ. Efficient calculation of vibrational magnetic dipole transition moments and rotational strengths. *Chem*

Phys Lett 1987, 133:21–26. doi:10.1016/0009–2614(87)80046–5

29. Yang D, Rauk A. Vibrational circular dichroism intensities by ab initio second-order Møller–Plesset vibronic coupling theory. *J Chem Phys* 1994, 100:7995. doi:10.1063/1.466792
30. Devlin FJ, Stephens PJ. Ab initio calculation of vibrational circular dichroism spectra of chiral natural products using MP2 force fields: camphor. *J Am Chem Soc* 1994, 116:5003–5004. doi:10.1021/ja00090a062
31. Abbate S, Castiglioni E, Gangemi F, Gangemi R, Longhi G. NIR-VCD, vibrational circular dichroism in the near-infrared: Experiments, theory and calculations. *Chirality* 2009, 21:S242–S252. doi:10.1002/chir.20805
32. Bak KL, Bludsky O, Jorgensen P. Ab initio calculations of anharmonic vibrational circular dichroism intensities of trans-2,3-dideuteriooxirane. *J Chem Phys* 1995, 103:10548–10555. doi:10.1063/1.469838
33. He Y, Cao X, Nafie LA, Freedman TB. Ab initio VCD calculation of a transition-metal containing molecule and a new intensity enhancement mechanism for VCD. *J Am Chem Soc* 2001, 123:11320–11321. doi:10.1021/ja016218i
34. Nafie LA. Theory of vibrational circular dichroism and infrared absorption: extension to molecules with low-lying excited electronic states. *J Phys Chem A* 2004, 108:7222–7231. doi:10.1021/jp0499124
35. Nicu VP, Baerends EJ. Robust normal modes in vibrational circular dichroism spectra. *Phys Chem Chem Phys* 2009, 11:6107. doi:10.1039/b823558a
36. Nafie LA. Electron transition current density in molecules. 1. Non-Born−Oppenheimer theory of vibronic and vibrational transitions. *J Phys Chem A* 1997, 101:7826–7833. doi:10.1021/jp9706137
37. Freedman TB, Lee E, Nafie LA. Vibrational transition current density in (S)-methyl lactate: visualizing the origin of the methine-stretching vibrational circular dichroism intensity. *J Phys Chem A* 2000, 104:3944–3951. doi:10.1021/jp0005470
38. Bursi R, Devlin FJ, Stephens PJ. Vibrationally induced ring currents? The vibrational circular dichroism of methyl lactate. *J Am Chem Soc* 1990, 112:9430–9432. doi:10.1021/ja00181a076
39. Freedman TB, Cao X, Dukor RK, Nafie LA. Absolute configuration determination of chiral molecules in the solution state using vibrational circular dichroism. *Chirality* 2003, 15:743–758. doi:10.1002/chir.10287
40. Stephens PJ, Devlin FJ, Pan J. The determination of the absolute configurations of chiral molecules using vibrational circular dichroism (VCD) spectroscopy. *Chirality* 2008, 20:643–663. doi:10.1002/chir.20477
41. McCann J, Rauk A, Shustov GV, Wieser H, Yang D. Electronic and vibrational circular dichroism of model β-lactams: 3-methyl- and 4-methylazetidin-2-one. *Appl Spectrosc* 1996, 50:630–641.
42. Rauk A, Yang D. Vibrational circular dichroism and infrared spectra of 2-methyloxirane and trans-2,3-dimethyloxirane: ab initio vibronic coupling theory with the 6-31G*(0.3) basis set. *J Phys Chem* 1992, 96:437–446. doi:10.1021/j100180a081
43. Rauk A, Eggimann T, Wieser H, Yang D. The infrared spectrum of 2-methylaziridine from scaled ab initio force fields. *Can J Chem* 1992, 70:464–477. doi:10.1139/v92–067
44. Rode JE, Dobrowolski JC. Density functional IR, Raman, and VCD spectra of halogen substituted β-lactams. *J Mol Struct* 2003, 651–653:705–717. doi:10.1016/S0022–2860(03)00121–2
45. Vass E, Hollósi M, Forró E, Fülöp F. VCD spectroscopic investigation of enantiopure cyclic β-lactams obtained through lipolase-catalyzed enantioselective ring-opening reaction. *Chirality* 2006, 18:733–740. doi:10.1002/chir.20312
46. Stephens PJ, Devlin FJ, Aamouche A. Determination of the structures of chiral molecules using vibrational circular dichroism spectroscopy. In: Hicks, JM ed., *Chirality: Physical Chemistry, ACS Symp. Series 810*. Washington, DC: American Chemical Society; 2002 p. 18–33.
47. Stephens P. Vibrational circular dichroism spectroscopy: a new tool for the stereochemical characterization of chiral molecules. In: Bultinck P, de Winter H, Langenaecker W, Tollenaere J. eds. *Computational Medicinal Chemistry for Drug Discovery*. New York: Marcel Dekker; 2003 p. 699–725.
48. Ashvar CS, Devlin FJ, Stephens PJ. Molecular structure in solution: an ab initio vibrational spectroscopy study of phenyloxirane. *J Am Chem Soc* 1999, 121:2836–2849. doi:10.1021/ja983302y
49. Fristrup P, Lassen PR, Johannessen C, Tanner D, Norrby P, Jalkanen KJ, Hemmingsen L. Direct determination of absolute configuration of methyl-substituted phenyloxiranes: combined experimental and theoretical approach. *J Phys Chem A* 2006, 110:9123–9129. doi:10.1021/jp060154m
50. Stephens PJ, Devlin FJ, Schürch S, Hulliger J. Determination of the absolute configuration of chiral molecules via density functional theory calculations of vibrational circular dichroism and optical rotation: The chiral alkane D_3-anti-trans-anti-trans-anti-trans-perhydrotriphenylene. *Theor Chem Acc* 2007, 119:19–28. doi:10.1007/s00214–006-0245–7
51. Stephens P, Devlin F, Villani C, Gasparrini F, Mortera SL. Determination of the absolute configurations of chiral organometallic complexes via density functional theory calculations of their vibrational circular dichroism spectra: the chiral chromium tricarbonyl complex of N-pivaloyl-tetrahydroquinoline.

Inorg Chim Acta 2008, 361:987–999. doi:10.1016/j.ica.2007.06.010

52. Freedman TB, Cao X, Young DA, Nafie LA. Density functional theory calculations of vibrational circular dichroism in transition metal complexes: identification of solution conformations and mode of chloride ion association for (+)-tris(ethylenediaminato)-cobalt(III). *J Phys Chem A* 2002, 106:3560–3565. doi:10.1021/jp015519b
53. Sato H, Taniguchi T, Nakahashi A, Monde K, Yamagishi A. Effects of central metal ions on vibrational circular dichroism spectra of tris-(β-diketonato)-metal(iii) complexes. *Inorg Chem* 2007, 46:6755–6766. doi:10.1021/ic070300i
54. Taniguchi T, Monde K. Spectrum-structure relationship in carbohydrate vibrational circular dichroism and its application to glycoconjugates. *Chem-Asian J* 2007, 2:1258–1266. doi:10.1002/asia.200700180
55. Bouř P, Andrushchenko V, Kabeláč M, Maharaj V, Wieser H. Simulations of structure and vibrational spectra of deoxyoctanucleotides. *J Phys Chem B* 2005, 109:20579–20587. doi:10.1021/jp051218g
56. Bouř P, Sopková J, Bednárová L, Maloň P, Keiderling TA. Transfer of molecular property tensors in cartesian coordinates: a new algorithm for simulation of vibrational spectra. *J Comput Chem* 1997, 18:646–659. doi:10.1002/(SICI)1096–987X(19970415)18:5<646::AID-JCC6>3.0.CO;2-N
57. Keiderling TA. Vibrational circular dichroism applications to conformational analysis of biomolecules. In: Fasman GD ed. *Circular Dichroism and the Conformational Analysis of Biomolecules*. New York: Plenum; 1996, 555–598.
58. Paterlini MG, Freedman TB, Nafie LA. Vibrational circular dichroism spectra of three conformationally distinct states and an unordered state of poly(L-lysine) in deuterated aqueous solution. *Biopolymers* 1986, 25:1751–1765. doi:10.1002/bip.360250915
59. Yasui SC, Keiderling TA. Vibrational circular dichroism of polypeptides. 8. Poly(lysine) conformations as a function of pH in aqueous solution. *J Am Chem Soc* 1986, 108:5576–5581. doi:10.1021/ja00278a035
60. Freedman TB, Nafie LA, Keiderling TA. Vibrational optical activity of oligopeptides. *Biopolymers* 1995, 37:265–279. doi:10.1002/bip.360370405
61. Barron LD, Hecht L, Bell AF. Vibrational Raman optical activity of biomolecules. In: Fasman GD ed. *Circular Dichroism and the Conformational Analysis of Biomolecules*. New York: Plenum; 1996, 653–695.
62. Kubelka J, Keiderling TA. Differentiation of β-sheet-forming structures: ab initio-based simulations of IR absorption and vibrational CD for model peptide and protein β-sheets. *J Am Chem Soc* 2001, 123:12048–12058. doi:10.1021/ja0116627
63. Singh RD, Keiderling TA. Vibrational circular dichroism of poly(gamma-benzyl-L-glutamate). *Biopolymers* 1981, 20:237–240. doi:10.1002/bip.1981.360200117
64. Silva RAGD, Kubelka J, Bouř P, Decatur SM, Keiderling TA. Site-specific conformational determination in thermal unfolding studies of helical peptides using vibrational circular dichroism with isotopic substitution. *Proc Natl Acad Sci USA* 2000, 97:8318–8323. doi:10.1073/pnas.140161997
65. Bouř P, Kubelka J, Keiderling TA. Simulations of oligopeptide vibrational CD: effects of isotopic labeling. *Biopolymers* 2000, 53:380–395. doi:10.1002/(SICI)1097–0282(20000415)53:5<380::AID-BIP3>3.0.CO;2-R
66. Huang R, Kubelka J, Barber-Armstrong W, Silva RAGD, Decatur SM, Keiderling TA. Nature of vibrational coupling in helical peptides: an isotopic labeling study. *J Am Chem Soc* 2004, 126:2346–2354. doi:10.1021/ja037998t
67. Kubelka J, Huang R, Keiderling TA. Solvent effects on IR and VCD Spectra of helical peptides: DFT-based static spectral simulations with explicit water. *J Phys Chem B* 2005, 109:8231–8243. doi:10.1021/jp0506078
68. Kubelka J, Silva RAGD, Keiderling TA. Discrimination between peptide 3_{10}- and α-helices. Theoretical analysis of the impact of α-methyl substitution on experimental spectra. *J Am Chem Soc* 2002, 124:5325–5332. doi:10.1021/ja012685o
69. Bouř P, Keiderling TA. Structure, spectra and the effects of twisting of β-sheet peptides. A density functional theory study. *J Mol Struc-Theochem* 2004, 675:95–105. doi:10.1016/j.theochem.2003.12.046
70. Hilario J, Kubelka J, Keiderling TA. Optical spectroscopic investigations of model β-sheet hairpins in aqueous solution. *J Am Chem Soc* 2003, 125:7562–7574. doi:10.1021/ja030039e
71. Bouř P, Keiderling TA. Vibrational spectral simulation for peptides of mixed secondary structure: method comparisons with the Trpzip model hairpin. *J Phys Chem B* 2005, 109:23687–23697. doi:10.1021/jp054107q
72. Perczel A, Hollósi M. Turns. In: Fasman GD ed. *Circular Dichroism and the Conformational Analysis of Biomolecules*. New York: Plenum; 1996, 285–380.
73. Vass E, Hollósi M, Besson F, Buchet R. Vibrational spectroscopic detection of beta- and gamma-turns in synthetic and natural peptides and proteins. *Chem Rev* 2003, 103:1917–1954. doi:10.1021/cr000100n
74. Borics A, Murphy RF, Lovas S. Optical spectroscopic elucidation of beta-turns in disulfide bridged cyclic tetrapeptides. *Biopolymers* 2007, 85:1–11. doi:10.1002/bip.20593
75. Kim J, Kapitán J, Lakhani A, Bouř P, Keiderling T. Tight β-turns in peptides. DFT-based study of infrared absorption and vibrational circular dichroism for various conformers including

solvent effects. *Theor Chem Acc* 2008, 119:81–97. doi:10.1007/s00214–006-0183–4

76. Cianciosi SJ, Spencer KM, Freedman TB, Nafie LA, Baldwin JE. Synthesis and gas-phase vibrational circular dichroism of (+)-(*S*,*S*)-cyclopropane-1,2–2H2. *J Am Chem Soc* 1989, 111:1913–1915. doi:10.1021/ja00187a074
77. Freedman TB, Spencer KM, Ragunathan N, Nafie LA, Moore JA, Schwab JM. Vibrational circular dichroism of (*S*,*S*)-[2,3–2H2]oxirane in the gas phase and in solution. *Can J Chem* 1991, 69:1619–1629. doi:10.1139/v91–237
78. Schlosser D, Devlin F, Jalkanen K, Stephens P. Vibrational circular dichroism of matrix-isolated molecules. *Chem Phys Lett* 1982, 88:286–291. doi:10.1016/0009–2614(82)87089–9
79. Henderson DO, Polavarapu PL. Fourier transform infrared vibrational circular dichroism of matrix-isolated molecules. *J Am Chem Soc* 1986, 108:7110–7111. doi:10.1021/ja00282a049
80. Tarczay G, Magyarfalvi G, Vass E. Towards the determination of the absolute configuration of complex molecular systems: matrix isolation vibrational circular dichroism study of (*R*)-2-amino-1-propanol. *Angew Chem Int Edit* 2006, 45:1775–1777. doi:10.1002/anie.200503319
81. Pohl G, Perczel A, Vass E, Magyarfalvi G, Tarczay G. A matrix isolation study on Ac-Gly-NHMe and Ac-L-Ala-NHMe, the simplest chiral and achiral building blocks of peptides and proteins. *Phys Chem Chem Phys* 2007, 9:4698–4708. doi:10.1039/b705098d
82. Pohl G, Perczel A, Vass E, Magyarfalvi G, Tarczay G. A matrix isolation study on Ac-L-Pro-NH_2: a frequent structural element of β- and γ-turns of peptides and proteins. *Tetrahedron* 2008, 64:2126–2133. doi:10.1016/j.tet.2007.12.037
83. Tarczay G, Góbi S, Vass E, Magyarfalvi G. Model peptide-water complexes in Ar matrix: complexation induced conformation change and chirality transfer. *Vib Spectrosc* 2009, 50:21–28. doi:10.1016/j.vibspec.2008.07.007
84. Nicu VP, JN, Baerends EJ. Effects of complex formation on vibrational circular dichroism spectra. *J Phys Chem A* 2008, 112:6978–6991. doi:10.1021/jp710201q
85. Jalkanen K, Degtyarenko I, Nieminen R, Cao X, Nafie L, Zhu F, Barron L. Role of hydration in determining the structure and vibrational spectra of L-alanine and N-acetyl L-alanine N′-methylamide in aqueous solution: a combined theoretical and experimental approach. *Theor Chem Acc* 2008, 119:191–210. doi:10.1007/s00214–007-0361-z
86. Chipman DM. Reaction field treatment of charge penetration. *J Chem Phys* 2000, 112:5558–5565. doi:10.1063/1.481133
87. Cancès E, Mennucci B. Comment on 'Reaction field treatment of charge penetration'. *J Chem Phys* 2000, 112:5558. *J Chem Phys* 2001, 114:4744–4745. doi:10.1063/1.1349091
88. Cossi M, Scalmani G, Rega N, Barone V. New developments in the polarizable continuum model for quantum mechanical and classical calculations on molecules in solution. *J Chem Phys* 2002, 117:43–54. doi:10.1063/1.1480445
89. Tomasi J, Mennucci B, Cammi R. Quantum mechanical continuum solvation models. *Chem Rev* 2005, 105:2999–3094. doi:10.1021/cr9904009
90. Bürgi T, Vargas A, Baiker A. VCD spectroscopy of chiral cinchona modifiers used in heterogeneous enantioselective hydrogenation: conformation and binding of non-chiral acids. *J Chem Soc, Perkin Trans. 2* 2002, (9):1596–1601. doi:10.1039/b203251a
91. Rode JE, Dobrowolski JC. VCD technique in determining intermolecular H-bond geometry: a DFT study. *J Mol Struc-Theochem* 2003, 637:81–89. doi:10.1016/S0166–1280(03)00366-X
92. Dong X, Zhou Z, Liu S, Gong X. Theoretical study of chiral discrimination in the hydrogen bonding complexes of lactic acid and hydrogen peroxide. *J Mol Struc-Theochem* 2005, 718:9–15. doi:10.1016/j.theochem.2004.10.053
93. Sadlej J, Dobrowolski JC, Rode JE, Jamroz MH. DFT study of vibrational circular dichroism spectra of d-lactic acid–water complexes. *Phys Chem Chem Phys* 2006, 8:101–113. doi:10.1039/b509351a
94. Losada M, Xu Y. Chirality transfer through hydrogen-bonding: experimental and ab initio analyses of vibrational circular dichroism spectra of methyl lactate in water. *Phys Chem Chem Phys* 2007, 9:3127–3135. doi:10.1039/b703368k
95. Debie E, Jaspers L, Bultinck P, Herrebout W, Veken BVD. Induced solvent chirality: a VCD study of camphor in $CDCl_3$. *Chem Phys Lett* 2008, 450:426–430. doi:10.1016/j.cplett.2007.11.064
96. Losada M, Tran H, Xu Y. Lactic acid in solution: investigations of lactic acid self-aggregation and hydrogen bonding interactions with water and methanol using vibrational absorption and vibrational circular dichroism spectroscopies. *J Chem Phys* 2008, 128:014508–11. doi:10.1063/1.2806192
97. Yang G, Xu Y. Probing chiral solute-water hydrogen bonding networks by chirality transfer effects: a vibrational circular dichroism study of glycidol in water. *J Chem Phys* 2009, 130:164506–9. doi:10.1063/1.3116582
98. Debie E, Bultinck P, Herrebout W, Veken BVD. Solvent effects on IR and VCD spectra of natural products: an experimental and theoretical VCD study of pulegone. *Phys Chem Chem Phys* 2008, 10:3498–3508. doi:10.1039/b801313f

99. Nicu VP, Debie E, Herrebout W, Veken BVD, Bultinck P, Baerends EJ. A VCD robust mode analysis of induced chirality: the case of pulegone in chloroform. *Chirality* 2009, 21:S287–S297. doi:10.1002/chir.20817
100. Zehnacker A, Suhm MA. Chirality recognition between neutral molecules in the gas phase. *Angew Chem Int Edit* 2008, 47:6970–6992. doi:10.1002/anie.200800957
101. Sadlej J, Dobrowolski JC, Rode JE. VCD spectroscopy as a novel probe for chirality transfer in molecular interactions. *Chem Soc Rev* 2010, 39:1478–1488. doi:10.1039/b915178h
102. Ma S, Freedman TB, Cao X, Nafie LA. Two-dimensional vibrational circular dichroism correlation spectroscopy: pH-induced spectral changes in l-alanine. *J Mol Struct* 2006, 799:226–238. doi:10.1016/j.molstruc.2006.03.039

FURTHER READING

Hicks JM, ed. *Chirality: Physical Chemistry, ACS Symp. Series 810*. Washington, DC: American Chemical Society; 2002.

Busch KW, Busch MA, eds. *Chiral Analysis*. Elsevier Science; 2006.

Barron LD. *Molecular Light Scattering and Optical Activity*. 2nd ed. Cambridge University Press; 2004.

Berova N, Nakanishi K, Woody RW, eds. *Circular Dichroism: Principles and Applications*. Wiley-VCH; 2000.

